DOT/FAA/AR-04/40,P4

Office of Aviation Research
Washington, D.C. 20591

Explicit Finite Element Modeling of Multilayer Composite Fabric for Gas Turbine Engine Containment Systems

Part 4: Model Simulation for Ballistic Tests, Engine Fan Blade-Out, and Generic Engine

November 2004

Final Report

This document is available to the U.S. public through the National Technical Information Service (NTIS), Springfield, Virginia 22161.

U.S. Department of Transportation
Federal Aviation Administration

NOTICE

Technical Report Documentation Page

1. Report No.	2. Government Accession No.	3. Recipient's Catalog No.
DOT/FAA/AR-04/40,P4		

4. Title and Subtitle	5. Report Date
EXPLICIT FINITE ELEMENT MODELING OF MULTILAYER COMPOSITE FABRIC FOR GAS TURBINE ENGINE CONTAINMENT SYSTEMS PART 4: MODEL SIMULATION FOR BALLISTIC TESTS, ENGINE FAN BLADE-OUT, AND GENERIC ENGINE	November 2004
	6. Performing Organization Code
7. Author(s)	8. Performing Organization Report No.
Reha Gomuc	21-12288
9. Performing Organization Name and Address	10. Work Unit No. (TRAIS)
Honeywell Engines, Systems & Services 111 S. 34th Street, P.O. Box 52181 Phoenix, AZ 85072-2181	11. Contract or Grant No. 01-C-AW-ASU Subagreement 02-11
12. Sponsoring Agency Name and Address	13. Type of Report and Period Covered
U.S. Department of Transportation Federal Aviation Administration FAA William J. Hughes Technical Center Atlantic City International Airport, NJ 08405	Final Report 9/2001 – 5/2003
	14. Sponsoring Agency Code ANE-100

15. Supplementary Notes

The FAA William J. Hughes Technical Center COTR was Donald Altobelli.

16. Abstract

Honeywell Engines, Systems & Services (Phoenix, AZ) collaborated with Arizona State University (Tempe, AZ), SRI International (Menlo Park, CA), and NASA Glenn Research Center (Cleveland, OH) to develop a robust explicit finite element analysis modeling methodology for gas turbine engine containment systems using multilayer composite fabrics. Honeywell's role was to simulate ballistic tests using LS-DYNA to validate the fabric material models (Task 3) and to apply the methodologies developed during this program to an engine fan blade containment analysis (Task 4). In addition, Honeywell developed a generic model for demonstration purposes. This report describes the work performed and the results obtained.

17. Key Words	18. Distribution Statement
Aircraft Engine, Composite fabric, Material modeling, LS-DYNA, Fan containment, Kevlar, Zylon	This document is available to the public through the National Technical Information Service (NTIS) Springfield, Virginia 22161.

19. Security Classif. (of this report)	20. Security Classif. (of this page)	21. No. of Pages	22. Price
Unclassified	Unclassified	68	

Form DOT F1700.7 (8-72) Reproduction of completed page authorized

TABLE OF CONTENTS

LIST OF FIGURES

LIST OF TABLES

LIST OF ACRONYMS

FAA	Federal Aviation Administration
Honeywell	Honeywell Engines, Systems & Services
HP	Hewlett-Packard Company
IBM	International Business Machines
LLNL	Lawrence Livermore National Laboratory
LSTC	Livermore Software Technology Corporation
NASA GRC	NASA Glenn Research Center
SRI	SRI international

EXECUTIVE SUMMARY

Modeling a multilayer fabric composite for engine containment systems during a fan blade-out event has been a challenging task. Nonlinear transient (explicit) finite element analysis (FEA) has the greatest potential of any numerical approach available to industry for analysis of these events. Significant research is still required to overcome difficulties with numerical stability, material modeling (pre- and postfailure), and standardizing model methods to achieve accurate simulation of the complex interactions between individual components during these high-speed events. The primary focus of this research was to develop the methodology for testing, modeling, and analysis of a typical fan blade-out event in a multilayer fiber fabric composite containment system. ABAQUS finite element code was used to verify the basic material model (prefailure state) developed through laboratory testing. LS-DYNA was the primary modeling tool used in the explicit finite element analysis of ballistic events.

During the Fourth Federal Aviation Administration (FAA) Uncontained Engine Debris Characterization Modeling and Mitigation Workshop (held in May 2000 at SRI International, Menlo Park, CA), a representative of Honeywell Engines, Systems & Services presented the capability of modeling complicated engine hub-burst and fan blade-out events. Predicting most of the event with high confidence was shown. At the same time, SRI International presented their efforts on modeling the material characteristics within LS-DYNA and developing a new composite fiber material called Zylon® that appeared to be stronger, lighter, and more temperature resistant than Kevlar®. Both parties showed interest in each other's work, and both agreed they could benefit from each other if collaborative mechanisms could be arranged. After the workshop, Honeywell and SRI contacted each other and began talks of a joint project. The FAA, National Aeronautics and Space Administration (NASA) Glenn Research Center (GRC), and Arizona State University (ASU) were later invited into the discussion, resulting in this FAA-funded research under the Aircraft Catastrophic Prevention Program and the Airworthiness Assurance Center of Excellence Program.

The goal of this research was to use the technical strengths of Honeywell, SRI, NASA GRC, and ASU for developing a robust explicit FEA modeling methodology for the purposes mentioned above. Since the development of an experimental set of data to support the calibration of the FE models is essential, various experimental methods to measure material and structural response of the fabrics were conducted. NASA GRC under the NASA Aviation Safety Program, conducted a series of fabric engine containment ring tests that were used for modeling in this program.

Each member of the team took a leadership role and developed a comprehensive report describing the details of the research task and the findings. The complete FAA report is comprised of the following four separate reports (parts 1 through 4).

- Part 1: Static Tests and Modeling by Arizona State University Department of Civil Engineering
- Part 2: Ballistic Testing by NASA Glenn Research Center

- Part 3: Material Model Development and Simulation of Experiments by SRI International

- Part 4: Model Simulation for Ballistic Tests, Engine Fan Blade-Out, and Generic Engine by Honeywell Engines, Systems & Services

This report describes work performed under the AACE Cooperative Agreement No. 01-C-AW-ASU Subagreement 02-11 during the period September 2001 through May 2003 and the results of the analytical simulations.

Overall, the analytical results agreed well with the ballistic test results. Acceptable correlation was obtained between the simulation and ballistic test results for both Kevlar and Zylon materials, using a single shell-element layer simulating all the fabric layers. Both the energy absorption and the overall deflection behavior of the fabric systems were successfully simulated. Similar successful analysis-to-test correlations were also obtained when up to four layers of shell elements are used to model all fabric layers.

In addition, a full-scale engine fan blade-out event was successfully simulated using the fabric material models and developed analytical methodologies. Acceptable correlation was obtained between the simulation results and the engine containment test results, using the new Kevlar material model and the single shell layer modeling technique.

Based on the experience gained during the execution of the above simulations, a generic containment FE model, including fabric wraps, was created. This model provides LS-DYNA users with generic guidelines for modeling composite fabric wraps in impact containment-related applications. This generic model is provided on the CD-ROM version of the report. The sensitivity of the results of this type of analysis-to-analysis parameters and solution algorithms and to the program version and computer platform choices is also discussed.

1. INTRODUCTION.

1.1 PURPOSE.

This research effort was undertaken as a direct result of discussions from the Fourth Federal Aviation Administration (FAA) Uncontained Debris Characterization Modeling and Mitigation Workshop (held in May 2000 at SRI International). A team effort between government, academia, and industry was seen as an excellent opportunity to transition fabric modeling and testing research, which was being sponsored by the FAA Aircraft Catastrophic Failure Prevention program, into commercial aircraft.

1.2 BACKGROUND.

Composite fiber fabric wraps are widely used in the containment systems of aerospace gas turbine engines. Such systems have been found to be especially cost-effective for mitigating engine debris during a possible engine fan blade-out event. Compared against traditional metallic containment systems, these fabric wrap systems have very high strength per unit weight properties and are inexpensive to manufacture.

LS-DYNA is a commercial explicit finite element program widely used in the analysis of gas turbine engine rotor containment applications. This program has been successfully used at Honeywell Engines, Systems & Services as an analysis tool to design and optimize containment structures. Although there are challenges involved, due to the complexity of these types of analyses, many successful modeling experiences exist, especially for containment systems using metallic materials. On the other hand, the modeling and analysis of a typical fan blade-out event in a multilayer fiber fabric composite containment system has always been a difficult task, mainly due to the lack of accurate numerical modeling techniques and material formulations. To properly use the advantages of the fabric containment systems, it is necessary to have a robust finite element analysis modeling methodology that integrates the representative material behavior and the problem-specific analysis techniques. The resulting tool can then be used to analyze and optimize the performance of the fabric-based containment systems.

The primary focus of this research program was to address the technology gaps in this area and develop a robust modeling methodology for the analysis of fan blade-out event in a multilayer fabric containment system. Some of the specific program objectives are as follows.

- Couple the LS-DYNA modeling expertise of Honeywell with the material modeling capability of SRI, the ballistic testing capabilities of National Aeronautics and Space Administration (NASA) Glenn Research Center (GRC), and the experimental facilities and finite element analysis/modeling capabilities of Arizona State University.

- Incorporate the material model developed by SRI into the LS-DYNA modeling methodology developed by Honeywell and correlate against the results from controlled laboratory hardware tests and then develop new methodologies if necessary.

- Develop methodologies for numerical simulation of engine fan blade-out events with composite fiber fabric wraps using SRI's material model and Honeywell's LS-DYNA modeling methodology. Validate the methodologies using existing engine fan blade-out containment test results from Honeywell.

- Compare the efficiency of Kevlar® and Zylon® wraps through laboratory hardware tests and LS-DYNA analysis of the test coupons.

- Explore the potential of Zylon for future gas turbine engine containment systems.

This report describes the details of the work conducted by Honeywell to complete tasks 3 and 4. First, the ballistic tests were numerically modeled and simulated using the LS-DYNA code. The material model developed by SRI using the static test data obtained during task 1 was also incorporated into the modeling. Modifications were made to the material model until a reasonable correlation was obtained between simulations and the test data for both Kevlar and Zylon materials. Second, the resulting material model and the modeling techniques were used to model and simulate a recent fan blade-out containment test of a full-scale Honeywell turbofan engine to validate the approach. In addition, a generic containment model was also prepared to provide the LS-DYNA users with a generic guideline for modeling composite fabric wraps in impact containment applications.

Also included in this report is a brief discussion of the comparisons between a new Johnson-Cook material model developed by Lawrence Livermore National Laboratory (LLNL) and the conventional metallic material model used by Honeywell in impact-related applications.

2. NUMERICAL SIMULATION OF BALLISTIC TESTS (TASK 3).

2.1 OBJECTIVE.

The primary objective was to develop and calibrate the Kevlar and Zylon material models developed under this research program using ballistic test data.

2.2 ANALYTICAL PROCEDURE.

To achieve the above objective, Honeywell simulated the Kevlar and Zylon ballistic tests conducted at NASA GRC and compared the simulation results to the actual test results. The detailed steps for the correlation efforts are given below. Figure 2-1 schematically illustrates the overall process followed during the execution of task 3. Table 2-1 shows the fabric properties of the Kevlar 49 and Zylon AS that were tested. Only the light Zylon AS and Kevlar 49 are included in the analysis of this report.

1. The ballistic tests were conducted at NASA GRC, and the details of the test procedures and results are reported in Part 2 of this report [1].

2. A composite fabric material model code (common for Kevlar and Zylon) provided by SRI was compiled together with the standard LS-DYNA binary files to obtain the user-defined executable. The typical LS-DYNA input deck included the model file (finite element nodes and elements), the user-controlled material input parameters (different sets for Kevlar and Zylon), the contact file defining the contact types to be used, and the control parameters required to run the LS-DYNA code.

3. Each test condition was properly simulated by changing input parameters, such as the fabric material constants, the projectile speed, and the number of fabric layers. In the case where a test condition was repeated (two or more replicates), an average speed was used to simulate a nominal test result.

4. The calculated versus observed energy absorption was then compared for all tests of the same fabric to judge if the material code was acceptable or not. Iterations were made until acceptable correlation was obtained for both fabrics. The iterations mainly included the changes in internal formulation of the SRI material model fabrics and also LS-DYNA control parameters for contact representation between the fabric and the projectile.

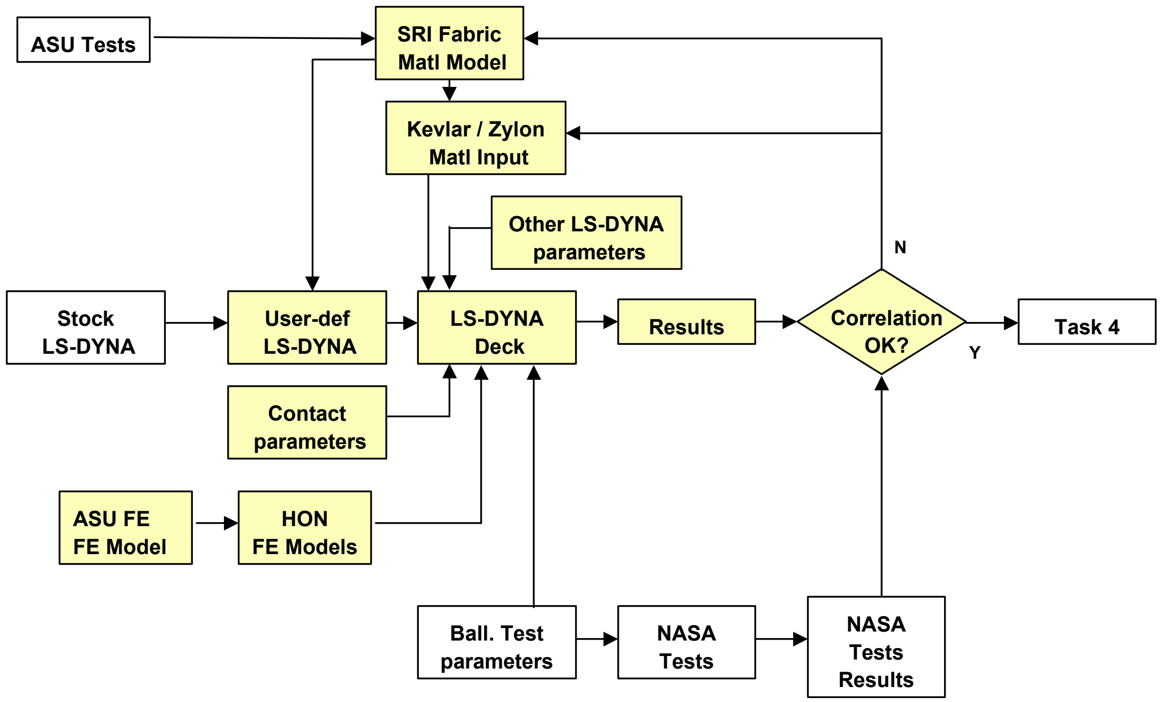

FIGURE 2-1. OVERALL PROCEDURE FOR THE NUMERICAL SIMULATION OF BALLISTIC TESTS

TABLE 2-1. FABRIC PROPERTIES

		Zylon AS Poly-benzobisoxazole		Kevlar-49 P-Aramid
		Light	Heavy	Standard
Volume Density	(g/cm^3)	1.54	1.54	1.44
Yarn Denier (measured)	(g/9km)	500	1500	1490
Yarn Linear Density	(mg/cm)	0.556	1.654	1.656
Yarn Count	(yarns/in)	35×35	17×17	17×17
Yarn Count	(yarns/cm)	13.8×13.8	6.7×6.7	6.7×6.7
Fabric Ply Thickness	(mm)	0.21	0.28	0.28
Fabric Areal Density	(g/cm^2)	0.01575	0.0223	0.02275
Degree of Crimp Warp Yarns	(%)	3.1	2.2	1.1
Degree of Crimp Fill Yarns	(%)	0.6	0.9	0.8

2.3 FINITE ELEMENT MODEL DESCRIPTION.

The ballistic test specimen(s) consisted of a thick steel cylinder welded on a plate, as shown in figure 2-2. For each individual test, the composite fabric was wrapped around this cylinder. A local window was machined out of the cylinder to provide access for the fabric wrap from the inside of the cylinder. The whole setup was inclined 15 degrees with respect to the horizontal plane such that the projectile could be shot directly into the exposed wrap area without interference from the rest of the cylinder.

FIGURE 2-2. BALLISTIC TEST SETUP AT NASA GRC

In the test samples, the composite fabric wraps were flat at the local opening of the cylinder, since there was no physical support to force the wraps to follow the curvature of the cylinder. In the finite element model, the shell simulating the fabric wraps follows the curvature of the cylinder even at the open area, as shown in figure 2-3. This is more representative of an actual engine fan containment structure where the fabric layers are always supported by a thin metallic or composite support layer. However, further comparison of the results with flat and curved modeling of the fabric at the opening did not reveal considerable differences.

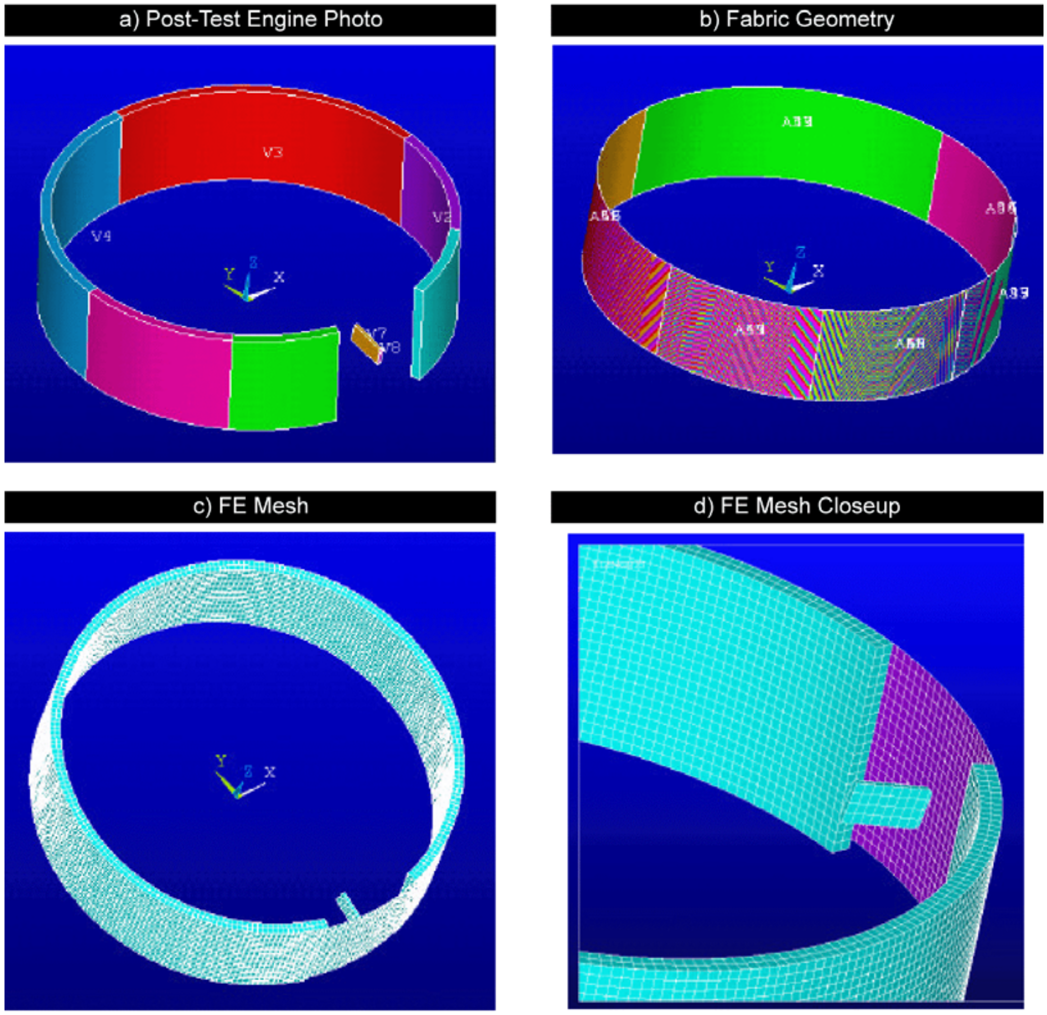

G03-201-3

FIGURE 2-3. BALLISTIC TEST FINITE ELEMENT MODEL

The following nomenclature was used to identify the fabric modeling used:

Total number of fabric layers simulated, $n = k \times m$

Where k is the number of shell-element layers physically modeled, and m is the number of composite fabric layers simulated per each shell. For example, the simulation 2×4 means that there was a total of eight layers of fabric wrapped around the cylinder during the test, and that the finite element modeling was done with two shell-element layers each representing the thickness and properties of four physically wrapped layers.

Figure 2-4 schematically illustrates different ways a test case could have been simulated. For the example chosen, there are eight layers of fabric wraps that are physically tested. This test can be simulated theoretically by one of the combinations satisfying the relationship: $k \times m = 8$, namely, 1×8, 2×4, 4×2, or 8×1. The primary focus of this program was to be able to simulate all the fabric layers by a single shell-element layer (1 × 8 in the given example), representing the total thickness of the pack. It was assumed that the fundamentals of the material formulation was adequate for simulating a single fabric layer as well as multiple fabric layers, as long as the total thickness is well represented. In this program, both Kevlar and Zylon ballistic tests were, therefore, simulated by a single layer shell element, representing the total number of fabric layers tested (1 × *n*). There are obvious advantages of single shell layer modeling since it provides a computationally inexpensive way to simulate overall behavior of the containment system. It avoids computational complications mainly related to contact interactions between individual fabric layers when all layers are explicitly modeled as separate shells, especially if the large number of fabric layers typically used in the fan containment design systems is taken into consideration (>30 layers in some cases). On the other hand, the single layer modeling by nature does not have the capability to predict the number of penetrated (or failed) versus nonpenetrated fabric layers. In the engine containment design problems, this information is usually valuable because it relates to the available margin of the containment system. To investigate the current capability of modeling multiple shells within the LS-DYNA limitations and computational constraints, the Zylon ballistic tests were also modeled with remaining combinations, namely multiple shell-element layers, representing 1 to 24 layers of fabric each.

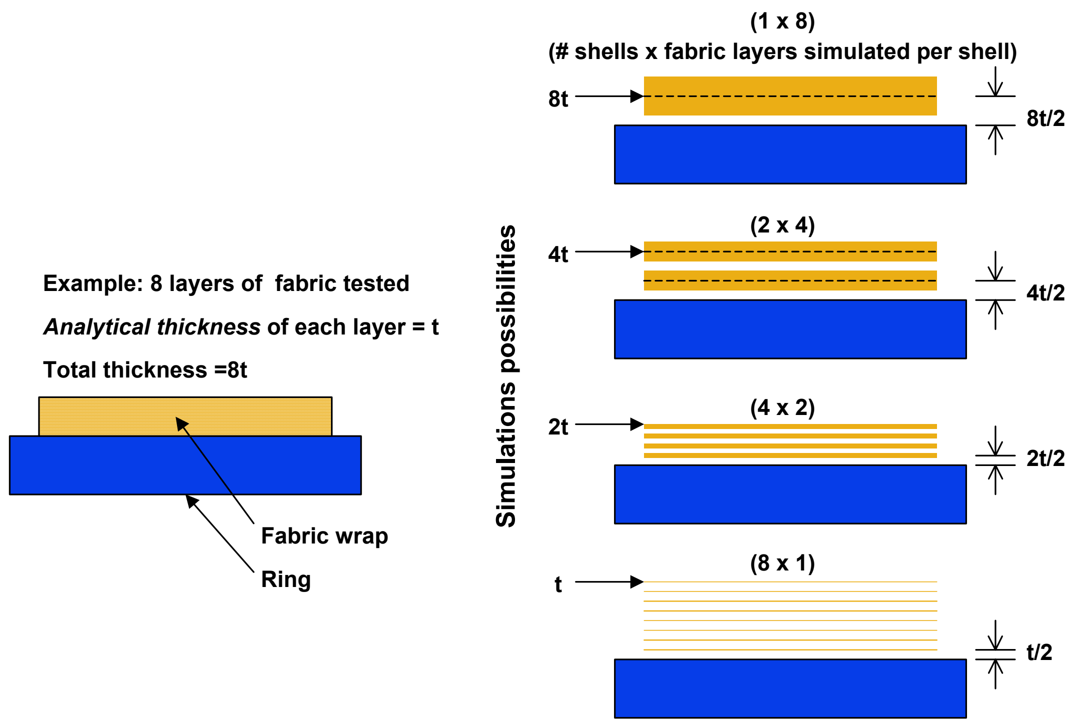

FIGURE 2-4. SCHEMATIC OF THE FABRIC SIMULATION TECHNIQUES

A common finite element practice is to model the shell elements at the mid-plane of the physical thin member (fabric in this case). Appropriate gaps between two consecutive shells and also between the ring and the first neighboring shell should then be provided for accurate contact computations, as shown in figure 2-4. Due to these required gap adjustments, the finite element model was unique for each simulated case.

It is important to note that when a shell-element layer is used to represent a fabric layer, the thickness of the shell is not the physical measured thickness of the fabric. The equivalent thickness, which is obtained by dividing the fabric areal density (g/cm^2 or lb/in^2) by the volume density from the manufacturer (g/cm^3 or lb/in^3), is more appropriate for numerical calculations. In addition, due to the fact that in a woven fabric structure, only the fibers along the axis of loading will react to the external load, only half of the fibers should be involved in the structural calculations. The shell-element thickness used in the model (analytical thickness) is, therefore, half of the calculated equivalent fabric thickness. Throughout this program, the Kevlar and Zylon shell-element analytical thicknesses were 0.00311 in. (0.0079 cm) and 0.00201 in. (0.0051 cm), respectively. Due to the fact that this analytical thickness adjustment will also reduce the weight of the modeled fabric, the density of the fabric was also adjusted in the analysis by multiplying by a factor of two in order to capture the representative dynamic behavior.

2.4 ANALYSIS TOOLS.

The same version of the LS-DYNA was used throughout this project, unless otherwise specified. This type of analysis, which involves high nonlinearities, failure, and contact interactions, is sensitive to program version, the computer platform used, the number of microprocessor(s) or type(s), and the operating system. A brief discussion on the effects of these parameters is given in section 6. To ensure consistency of the results, the following parameters were intentionally kept constant during this project:

- Standard LS-DYNA file: ls960_s_447_hp_102; LS-DYNA Version 960, Revision 477
- HP8000 Unix machines, with operating system Version 10.2, single processor, and single precision

2.5 ANALYSIS RESULTS.

The analysis matrices followed to simulate the ballistic test results are given in tables 2-2 and 2-3 for Kevlar and Zylon material, respectively. As outlined previously, only the single shell layer modeling was performed for Kevlar (first row of table 2-2), whereas single and multiple shell layer modeling were investigated for Zylon. After iterations, per figure 2-1, the final results obtained for both fabric materials were as reported in tables 2-2 and 2-3. These results were obtained using the latest version of the material model code dated 10-08-2002. The material model code was then kept unchanged throughout the rest of the project, including work conducted in task 4. Minor adjustments to the user-input time constant parameter were made to obtain the best correlation possible to the overall test results. The specifics of the material time constant are discussed by SRI in Part 3 of this report [2]. The optimal value of this parameter for Kevlar and Zylon was 0.008 and 0.002, respectively. Once the optimal values were determined, they were kept constant throughout the analyses performed in tasks 3 and 4. The user-defined material input decks are given in appendix A.

TABLE 2-2. ANALYSIS MATRIX AND SUMMARY OF BALLISTIC TEST SIMULATION RESULTS FOR KEVLAR

Kevlar Ballistic Tests						
No. of Layers	1	2	4	8	16	24
Percent Energy Absorbed	11.0 11.6	34.6 36.6	10.0 11.9	16.6 17.1 20.4	37.9 47.4	55.9 69.5 78.3
LS-DYNA Simulations						
$k \times m$	1 × 1	1 × 2	1 × 4	1 × 8	1 × 16	1 × 24
Model ID	Model 231_1	Model 232_2	Model 222_4	Model 228_8	Model 230_16	Model 229_24
Prediction	19.2%	56.6%	9.5%	18.6%	43.2%	73.5%
			2 × 2 * *	2 × 4 * *	2 × 8 * *	2 × 12 * *
			4 × 1 * *	4 × 2 * *	4 × 4 * *	4 × 6 * *
				8 × 1 * *	8 × 2 * *	8 × 3 * *
					16 × 1 * *	12 × 2 * *
						24 × 1 * *

Notes:
$k \times m$ = no. of shells × no. of fabric layers simulated per shell. Prediction = predicted percent energy absorbed.
* = simulation not performed.

TABLE 2-3. ANALYSIS MATRIX AND SUMMARY OF BALLISTIC TEST SIMULATION RESULTS FOR ZYLON

Zylon Ballistic Tests					
No. of Layers	2	4	8	16	24
Percent Energy Absorbed	N/A	12.9 15.6	21.4 21.6 23.2 25.8	52.2	100.0 100.0
LS-DYNA Simulations					
$k \times m$	---	1×4	1×8	1×16	1×24
Model ID	---	model122_4	model128_8	model130_16	model129_24
Prediction	---	8.3%	19.4%	65.8%	99.0%
		2×2 model122_2 9.9%	2×4 model128_4 17.0%	2×8 model130_8 48.0%	2×12 model129_12 98.6%
		4×1 model122 9.3%	4×2 model128_2 18.0%	4×4 model130_4 44.4%	4×6 model129_6 98.9%
			8×1 model128 16.8%	8×2 model130_2 36.6%	8×3 model129_34 68.5%
				16×1 model130 33.3%	12×2 model129_2 55.2%
					24×1 model129 46.1%

Note:
$k \times m$ = no. of shells × no. of fabric layers simulated per shell.
Prediction = predicted percent energy absorbed.

A detailed summary of the test results and the analytical predictions is also given in appendix B. As already mentioned in section 2.2, some of the ballistic tests were repeated up to four times, resulting in some scatter in the results, which is expected from this type of experimental work. Part of this scatter is due to slightly different initial conditions for the individual tests. For example, there are three replicas for the eight-layer Kevlar test. Each of the tests has its own measured projectile mass and initial velocity, contributing to variation in impact energy values, and, therefore, affecting the exit velocity and energy. The initial velocity variation and the projectile mass variation in this example were 11 percent and 1 percent, respectively. The resulting exit velocity, exit energy, and absorbed energy variations were 10, 20, and 7 percent, respectively.

On the analytical side, it was not practical to simulate individual tests by adjusting the initial velocity and projectile mass; therefore, a single analysis was performed at a nominal initial kinetic energy level. In most cases, the initial test velocities were then updated by NASA GRC (due to further detailed data processing) after the completion of the simulation analysis. This resulted in further discrepancy between the test initial conditions and the corresponding simulation initial condition. For the example chosen, the simulation kinetic energy was deviating from individual test kinetic energies by 5 to 20 percent. To be able to compare the results from individual tests to a single nominal analysis result, the following adjustment was made: the predicted exit kinetic energy was scaled by the ratio of the initial energy of the analysis to the individual test initial energy. In this way, an exit kinetic energy prediction corresponding to each individual test condition was estimated for a more realistic comparison.

Figure 2-5 is reproduced from the NASA GRC test data to show the trends obtained during the tests. The energy absorbed by the fabric layers increased as the number of layers increased for all three fabrics tested. The material model creation and the analytical simulations were only conducted for light Zylon AS and Kevlar 49; the heavy Zylon was not studied. Zylon performed slightly better than Kevlar, especially for the cases having more than eight layers. The heavy Zylon outperformed both Kevlar and light Zylon for any number of layers. It should be noted that the areal weight of the heavy Zylon and Kevlar 49 were similar but the light Zylon AS was significantly less.

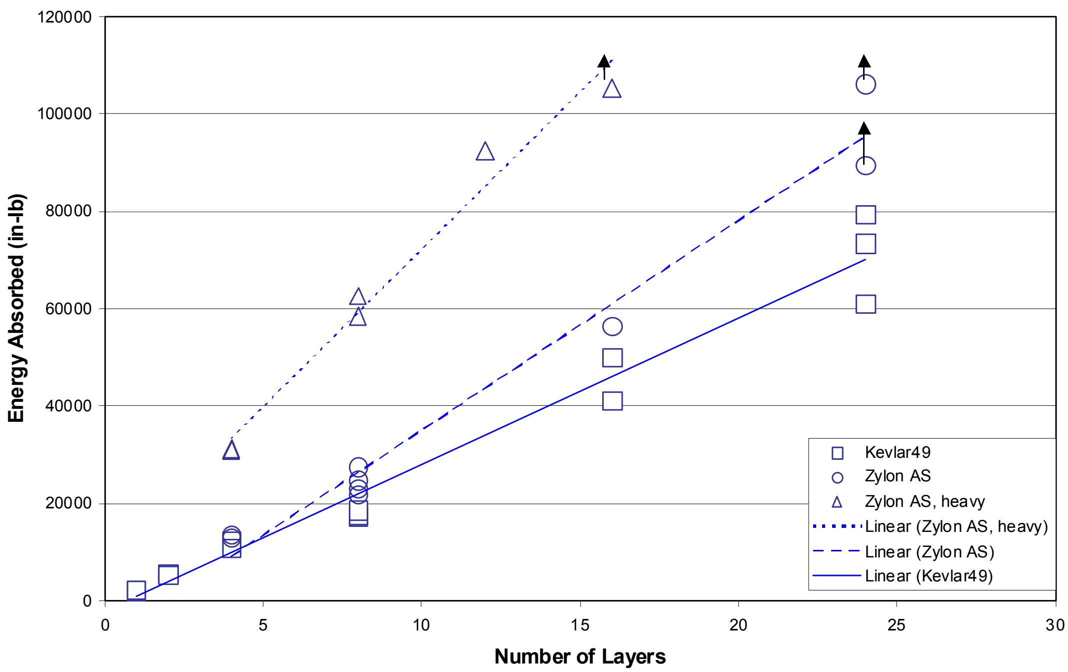

FIGURE 2-5. BALLISTIC TEST RESULTS (NASA GRC TEST DATA)

2.5.1 Kevlar Ballistic Test Simulations.

Table 2-2 also summarizes the percent energy absorbed during the simulation as well as the particular model used for reference (single shell-layer modeling only, $1 \times m$). The predicted percent energy absorption can be compared to observed energy absorption for each test given in table 2-2. The compilation of the analysis models and the results are also given in table B-1 of appendix B. Figure 2-6 shows the experimental results for Kevlar from figure 2-5, compared against the LS-DYNA simulation results. The overall correlation for the amount of energy absorbed was found to be acceptable for the range investigated. The energy absorption is a measurable parameter that can be used to judge the success of the simulation. However, to make a thorough judgment of the material modeling capability, other parameters, such as velocity and deceleration histograms during the penetration process, are desirable. LS-DYNA has the capability to provide the change in these parameters during the event, as shown in the velocity histogram in figure 2-7. The current ballistic testing technology provides only the information at the beginning and end of the event, and no measurements are available during the course of the event, to correlate with the analysis. Later in the program, some additional data processing work was performed by NASA GRC to obtain further position-time and deflection-time information on selected tests. Figure 2-8 shows an example where the position of the projectile was tracked on the high-speed camera throughout the event to better evaluate the overall behavior. Although this effort gave more information about the before and after impact conditions, there was not enough resolution during the impact portion for further comparison to analytical results.

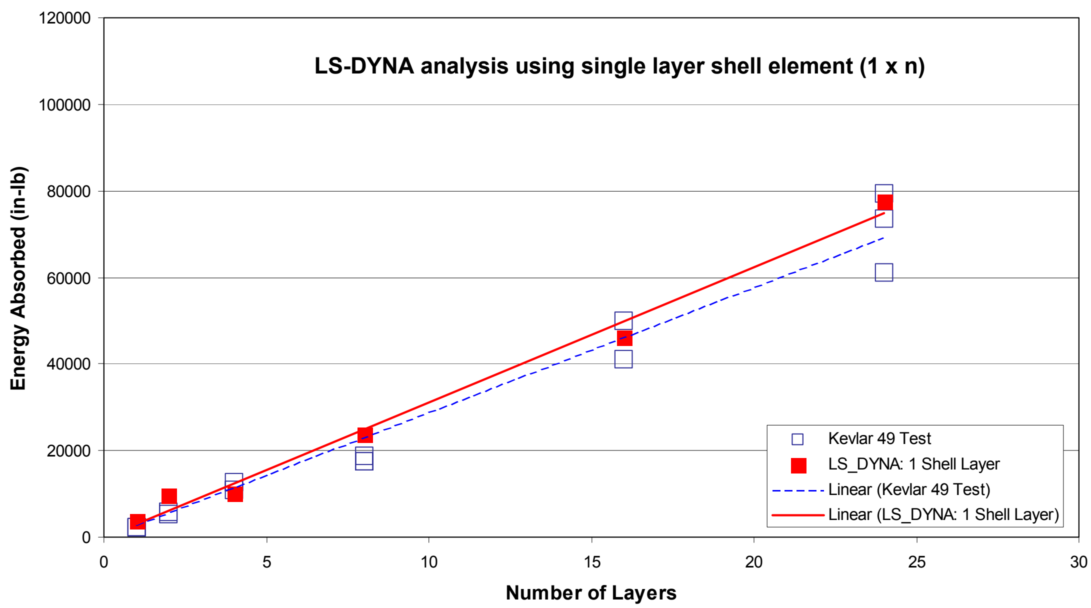

FIGURE 2-6. KEVLAR BALLISTIC TEST RESULTS VERSUS LS-DYNA PREDICTIONS

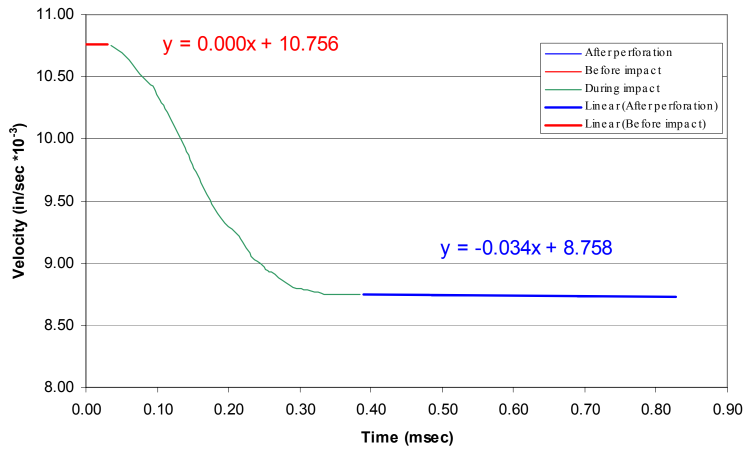

FIGURE 2-7. PROJECTILE VELOCITY HISTOGRAM DURING A 16-LAYER KEVLAR SIMULATION TEST

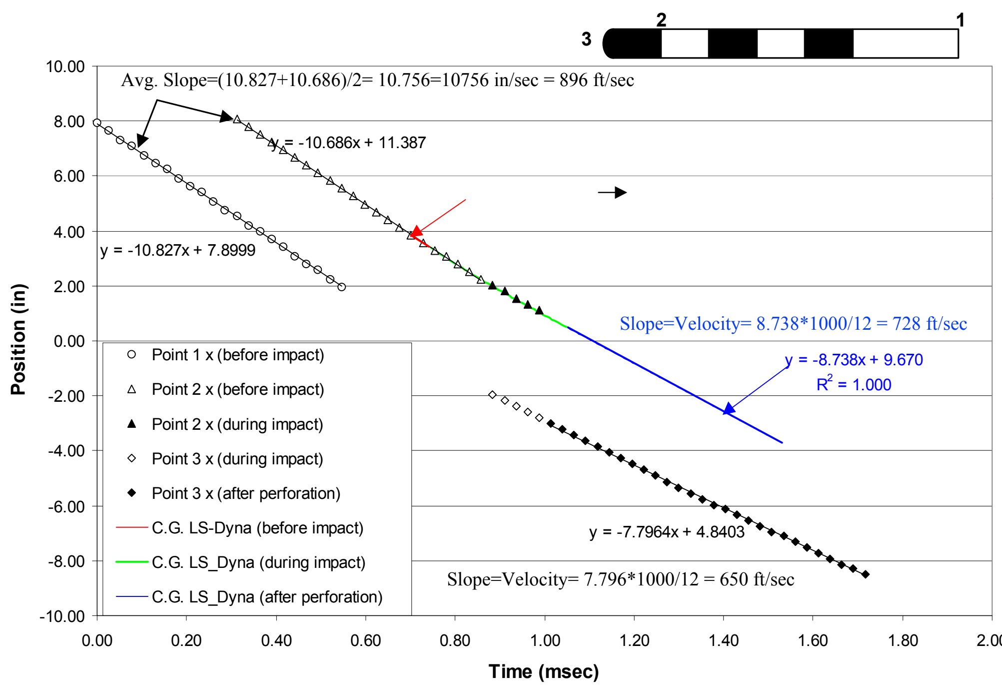

FIGURE 2-8. PROJECTILE POSITION HISTOGRAM DURING A 16-LAYER KEVLAR BALLISTIC TEST

LS-DYNA has more than the capability to predict the end result, it also provides the local and/or the overall deflection behavior during the event. Figure 2-9 shows the results from a 16-layer Kevlar test at the verge of the fragment penetration and the corresponding LS-DYNA analytical prediction. The deformed shape of the fabric and the interaction with the projectile can also be realistically simulated in addition to the energy absorption. More examples of the deformed shape comparisons are given in section 2.5.2, where the analytical results for Zylon are discussed. One particular piece of information that is useful to the engine containment designers is the maximum deflection of the fabric layers during the containment event, especially when the projectile is fully contained. This allows designers to adequately position the surrounding engine parts and accessories without safety concerns. An attempt was made to correlate the maximum deflection measured during a selected (16-layer Kevlar) test to the respective LS-DYNA prediction. Figure 2-10 compares the analytical versus experimental deflections for the test case shown in figure 2-9. It was concluded that LS-DYNA is able to predict the maximum fabric deflection reasonably well based on this limited data.

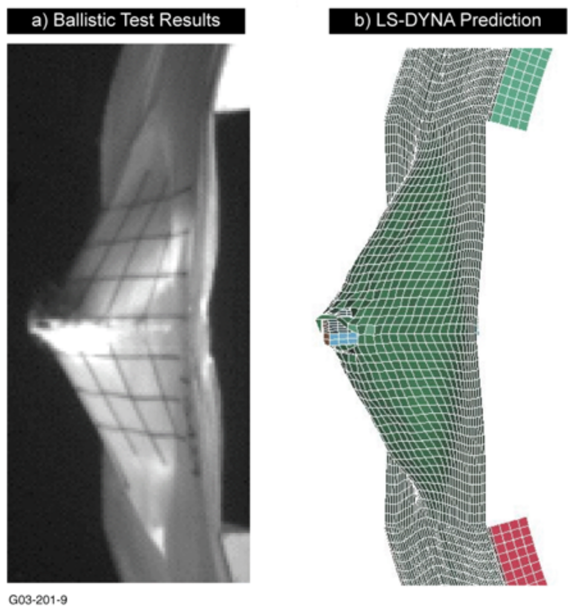

FIGURE 2-9. A 16-LAYER KEVLAR BALLISTIC TEST RESULT VERSUS LS-DYNA DEFLECTION PREDICTIONS

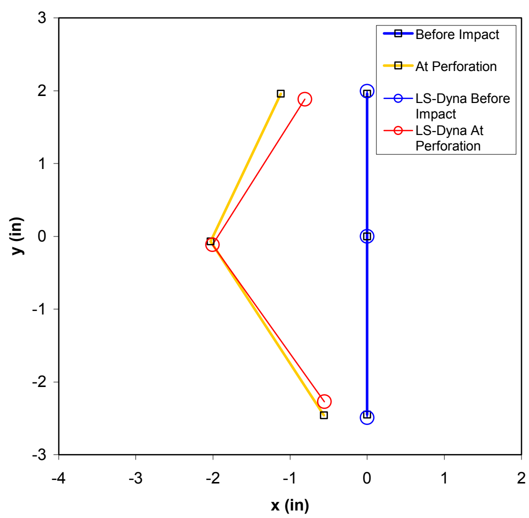

FIGURE 2-10. ANALYTICAL VERSUS EXPERIMENTAL DEFLECTIONS FOR A 16-LAYER KEVLAR BALLISTIC TEST

2.5.2 Zylon Ballistic Test Simulations.

Table 2-3 summarizes the percent energy absorbed during the Zylon test simulations. Similar to table 2-2, the first row of simulation is for single shell-layer modeling ($1 \times m$). The analytical results are also compiled in table B-2 of appendix B. Figure 2-11 shows the experimental test results for Zylon from figure 2-5, compared against the LS-DYNA simulation results. Once more, the overall correlation for the amount of energy absorbed was found to be acceptable for the range investigated. Figure 2-12 shows the correlation data for both Kevlar and Zylon, for energy absorbed (normalized per total areal density of the fabric system). This normalized parameter is useful in comparing the performance of fabrics with different densities. It can be concluded from figure 2-12, for example, that for the same weight of the wrapped containment system, Zylon can absorb more energy than Kevlar. This type of comparison will be further discussed in section 3. Figure 2-12 shows that the predictions agreed well with the test results for systems with more than eight layers of fabric. But for one to four layers, the predictions deviated by more than 50 percent.

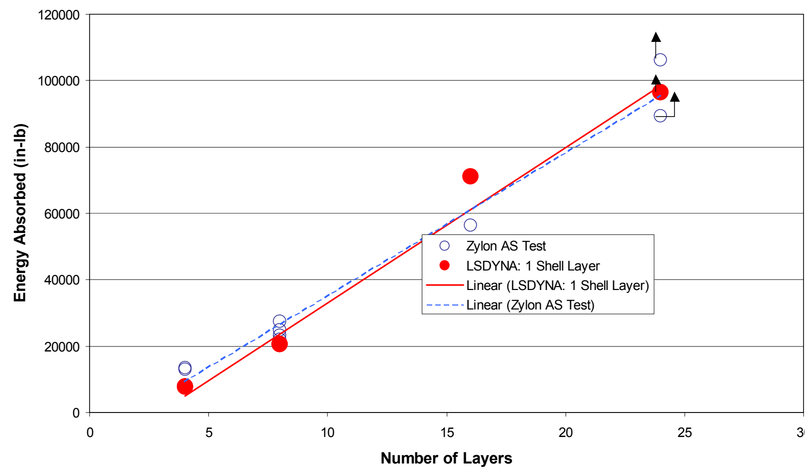

FIGURE 2-11. ZYLON BALLISTIC TEST RESULTS VERSUS LS-DYNA PREDICTIONS

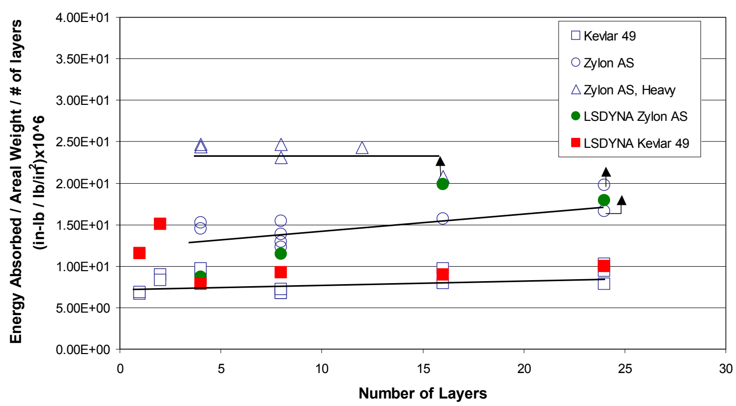

FIGURE 2-12. NORMALIZED BALLISTIC TEST RESULTS VERSUS LS-DYNA PREDICTIONS

Table 2-3 also includes the results with multiple shell modeling ($k \times m$) to simulate the actual fabric layers. The results indicate that for all fabric configurations (4 to 24 layers), the multiple shell-element modeling yields very similar results as the single shell-element modeling, when up to four shell-element layers are modeled. When more than four shell-element layers are used, the models failed to realistically simulate the test results. This is believed to be the result of solution divergence, due to numerical instabilities and complicated contact interactions between multiple layers. This correlation trend is also graphically illustrated in figures 2-13 and 2-14, where it is shown that the prediction capability rapidly decreased for models with more than four shell-element layers.

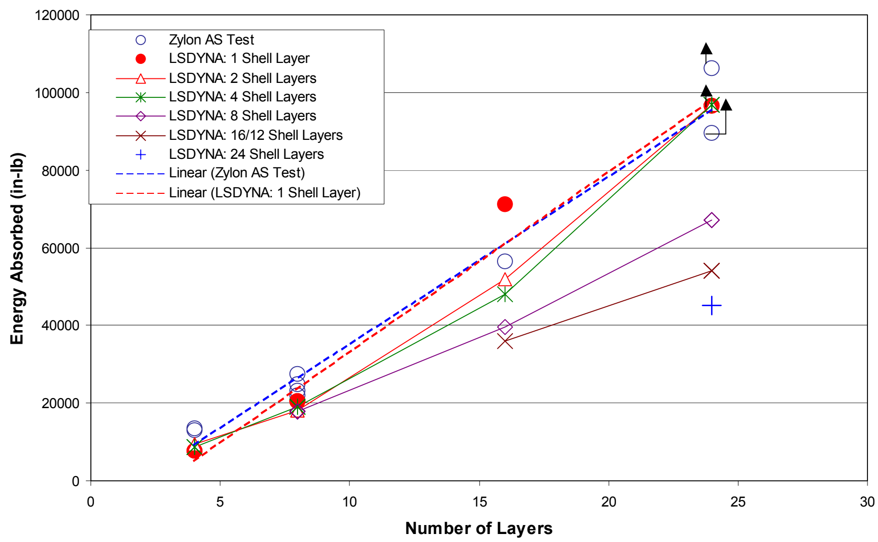

FIGURE 2-13. ZYLON BALLISTIC TEST RESULTS VERSUS LS-DYNA PREDICTIONS WITH MULTIPLE-LAYER SHELLS

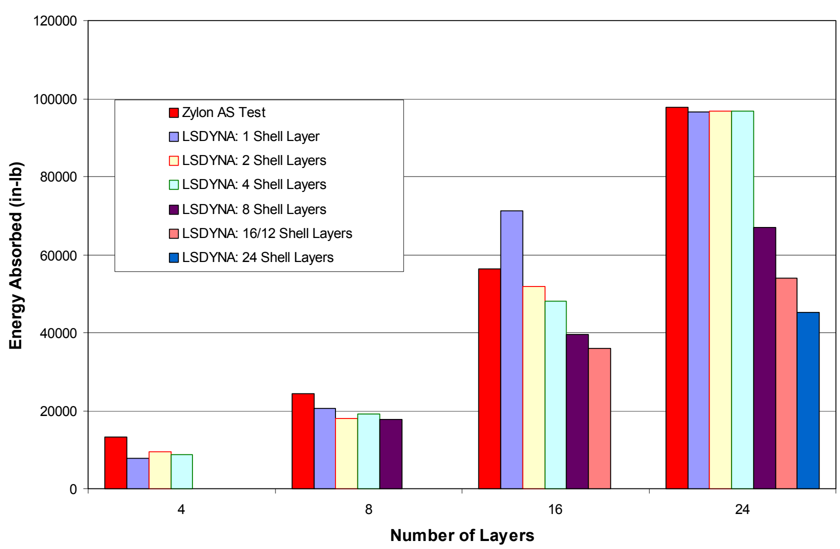

FIGURE 2-14. EFFECT OF MULTIPLE-LAYER FABRIC MODELING

In terms of the overall deflection behavior, some prediction-to-test comparisons are given in appendix C for the single shell-layer modeling technique. Similar to Kevlar, the Zylon deflection shape predictions matched very well against the high-speed camera test data. Figure 2-15 summarizes the effect of single- versus multiple-layer modeling techniques on deflection shape predictions. Similar to the energy absorption conclusion, a four-layer Zylon fabric system can be represented equally well with either one single shell-layer simulating four fabric layers ($4 = 1 \times 4$) or four shell layers simulating one fabric each ($4 = 4 \times 1$). Similarly, figure 2-16 summarizes the results of single- and multiple-layer modeling to simulate a 12-layer Zylon system. Once again, 1×24 and 4×6 models provided similar results and were successful in simulating the test behavior, whereas a 24×1 model failed to simulate the test behavior and diverged from the ideal representation towards the end of the simulation.

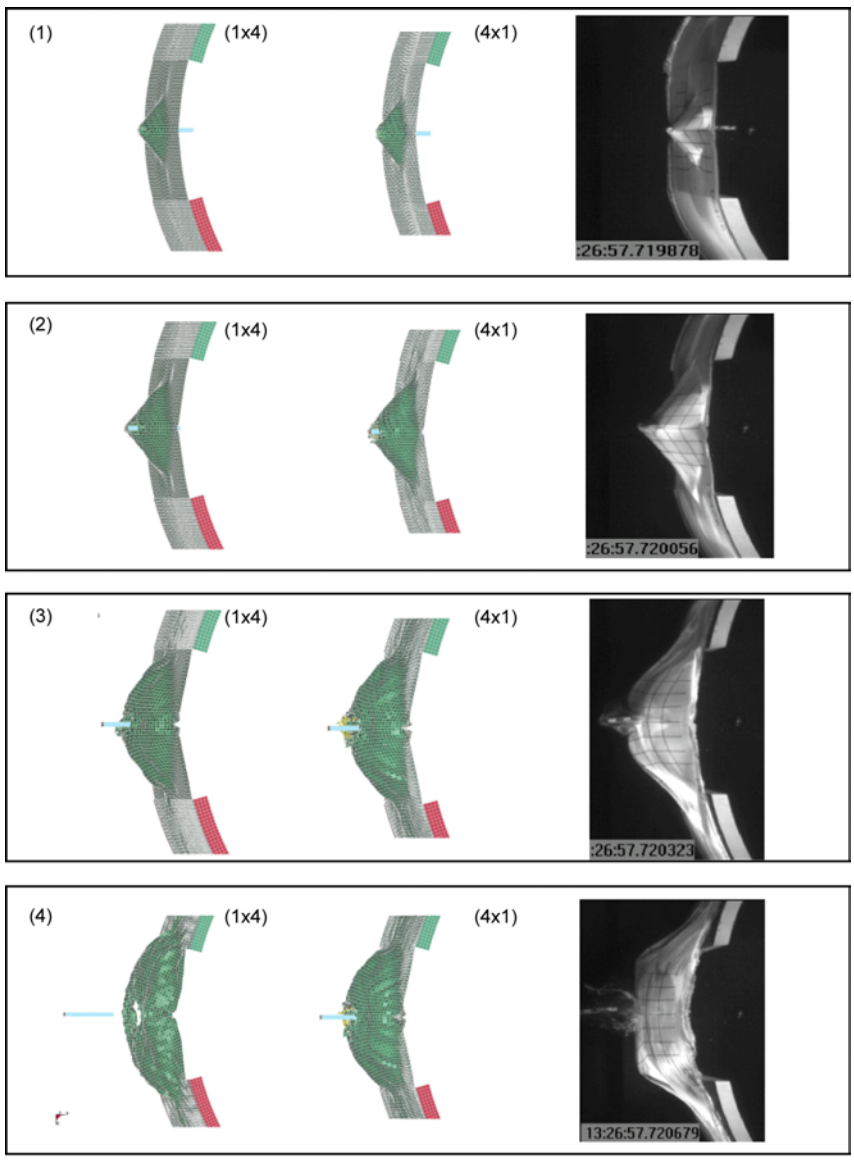

FIGURE 2-15. DEFLECTED SHAPES WITH SINGLE- VERSUS MULTIPLE-LAYER FABRIC MODELING (FOUR FABRIC LAYERS)

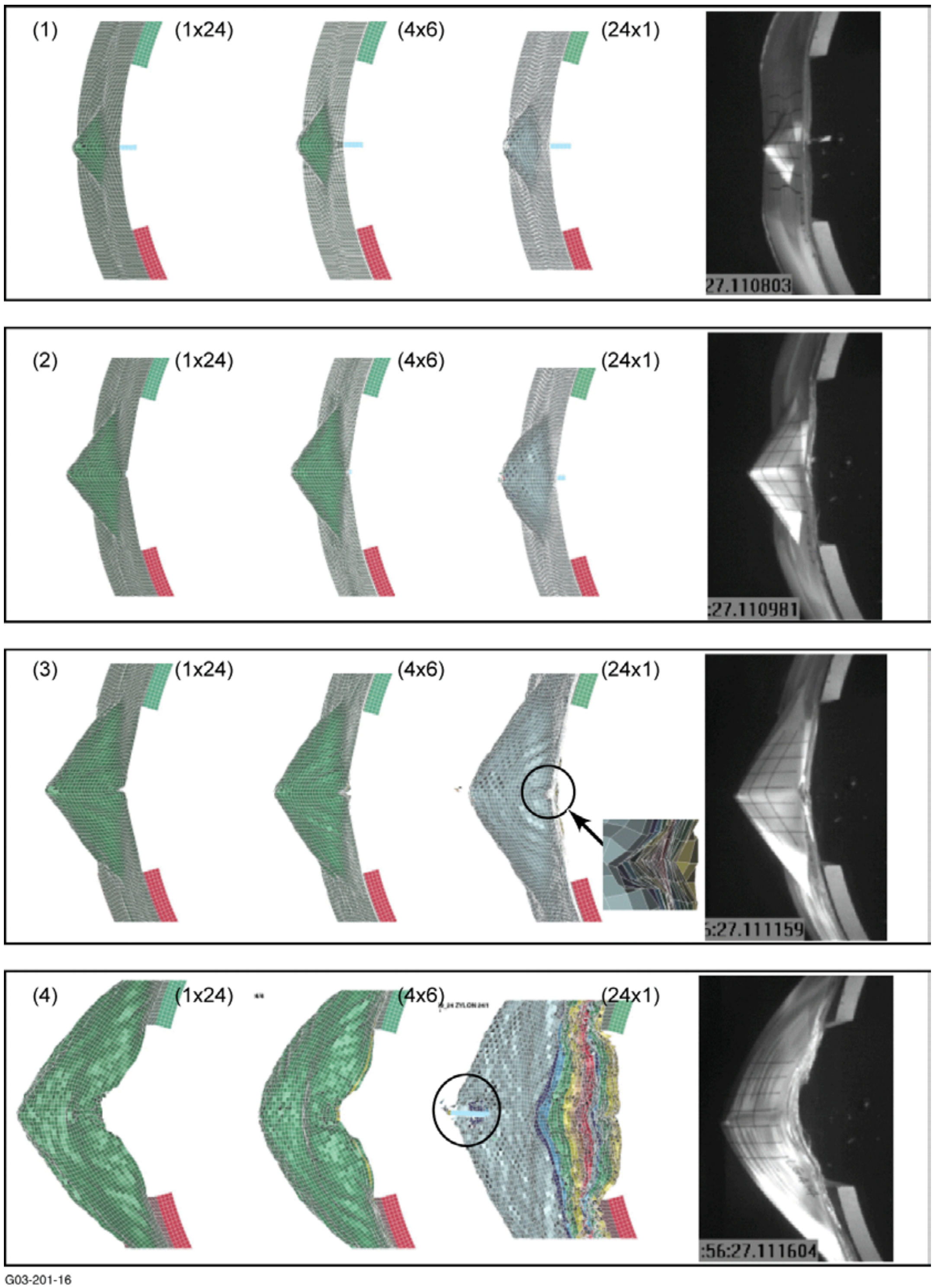

FIGURE 2-16. DEFLECTED SHAPES WITH SINGLE- VERSUS MULTIPLE-LAYER FABRIC MODELING (24 FABRIC LAYERS)

LS-DYNA also keeps track of the kinetic energy of the projectile during the impact event. Figures 2-17 and 2-18 provide the time histories of the kinetic energy for the previously mentioned 4-layer and 24-layer Zylon analyses, respectively. For all analyses that were successful in predicting the correct energy absorption and the overall deflections, the kinetic energy curves were similar. Whereas for the 24 × 1 case, the kinetic energy curve reflects the early failure, therefore supporting the poorly correlating result.

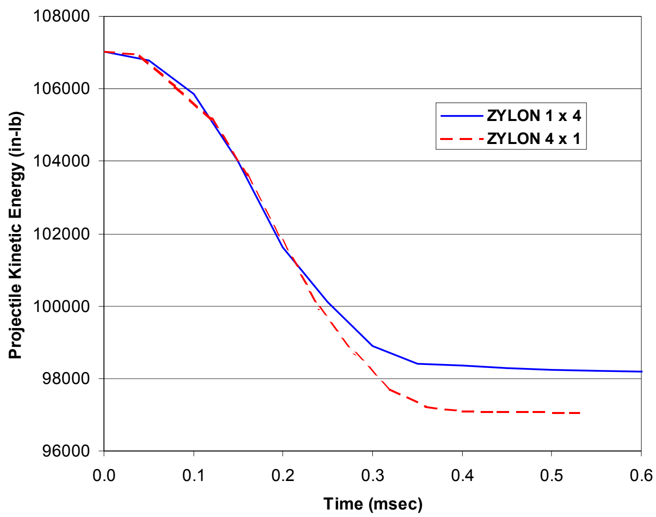

FIGURE 2-17. KINETIC ENERGY WITH SINGLE- VERSUS MULTIPLE-LAYER FABRIC MODELING (FOUR FABRIC LAYERS)

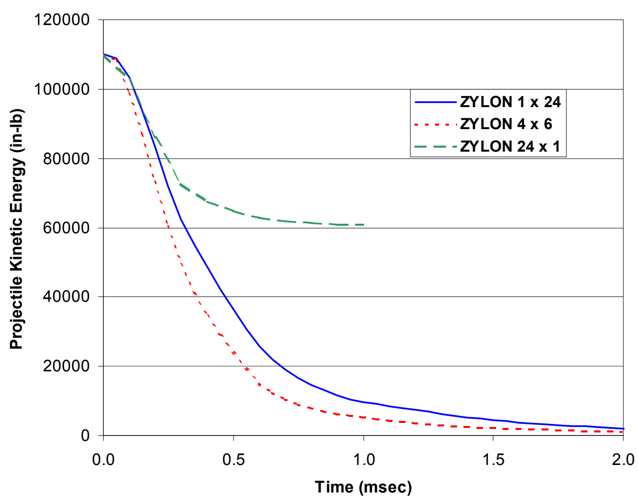

FIGURE 2-18. KINETIC ENERGY WITH SINGLE- VERSUS MULTIPLE-LAYER FABRIC MODELING (24 FABRIC LAYERS)

In conclusion, regardless of the number of total fabric layers to be simulated, the multiple-layer modeling techniques, using up to four layers, provided promising results for both energy absorption and the overall deflection behavior. Increasing the number of fabric layers caused divergence from the test data.

2.6 CONCLUSIONS.

The conclusions drawn from the task 3 results are summarized as follows:

- The new user-defined material model was successfully compiled within the LS-DYNA code. The same model is able to represent both Kevlar and Zylon material behavior, with separately provided material-specific constants. The model formulation is based on actual material data and provides a more realistic representation of the fabric behavior.

- The new material model is independent of the number of fabric layers, therefore providing the flexibility to model single- or multiple-fabric layers.

- Acceptable correlation was obtained between the simulation results and the ballistic test results for both Kevlar and Zylon using a single shell-element layer simulating all the fabric layers. Both the energy absorption and the overall deflection behavior of the fabric systems were successfully simulated. The relative simulations are able to depict the ballistic strength differences between Zylon and Kevlar.

- Promising successful analyses to test correlations are obtained when up to four layers of shell elements are used to model all fabric layers. Although good trends were observed up to four shell-element layers, the prediction capability was not satisfactory for modeling techniques using more than four shell-element layers. More work is needed to explore the limitations of modeling techniques involving high numbers of shell layers.

- The results are valid for the versions, the computer hardware, and the LS-DYNA parameters used.

- The mesh density was kept constant (0.25 inch (6.4 mm)) during this program. The possible effects on the results were not investigated.

3. NUMERICAL SIMULATION OF ENGINE FAN BLADE-OUT TEST (TASK 4).

3.1 OBJECTIVE.

The primary objective of this task was to validate the Kevlar and Zylon material models developed under this research program for use in LS-DYNA fan containment analyses.

3.2 ANALYTICAL PROCEDURE.

To achieve the above objective, Honeywell simulated an actual engine fan blade-out test using the material model and the analysis techniques developed during task 3 of this program. Figure 3-1 schematically illustrates the overall process followed during the execution of task 4. The detailed steps for the analytical efforts are given below.

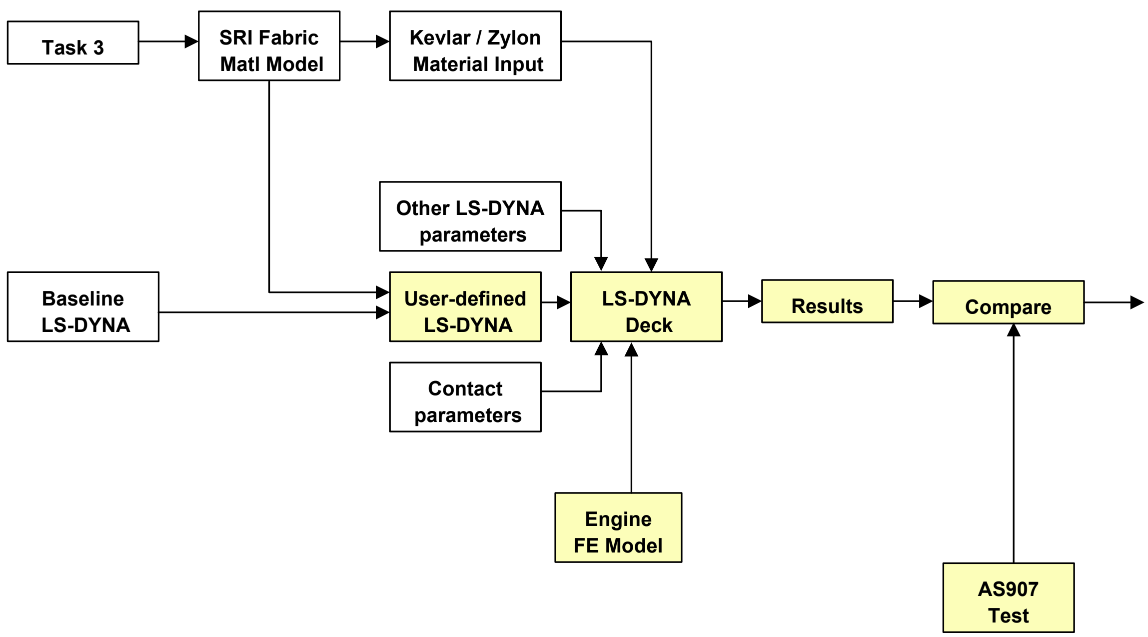

FIGURE 3-1. OVERALL PROCEDURE FOR THE ENGINE FAN BLADE-OUT SIMULATION

- A Honeywell turbofan engine model was chosen for validation of the techniques developed in task 3. The fan blade-out development test for this engine was conducted during 1999. A baseline 1999 LS-DYNA analysis predicted the results of this test using approximations related to the fabric material behavior due to a lack of material data.

- The composite fabric material model code, developed in previous tasks in this program, was used in the task 4 analyses to simulate the engine fan containment. The typical LS-DYNA input deck included the model file (finite element nodes and elements), the user-controlled material input parameters (see appendix A), the contact file defining the contact types to be used, and the LS-DYNA control parameters from task 3.

- The analytical predictions were then compared against the engine fan blade-out test results. The test results were captured in the form of engine hardware pictures taken before, during, and after the test, which allowed qualitative comparison of the ability of LS-DYNA to predict various failure modes against actual engine test results.

3.3 FAN BLADE-OUT TEST RESULTS.

During the development of the new Honeywell AS907 turbofan engine, a containment test was conducted on a full-scale engine to verify the fan blade-out containment and related design features prior to the official qualification test required by the FAA certification authorities. An overall view of this engine is shown in figure 3-2. The AS907 fan containment design incorporates composite fabric wraps with material properties equivalent to Kevlar. The number of layers required to adequately contain a possible fan blade separation were calculated using empirical Kevlar penetration design curves based on Honeywell experience with similar designs. The diameter of the AS907 containment system was comparable to the diameter of the ballistic test specimen in this project.

FIGURE 3-2. OVERALL VIEW OF THE HONEYWELL MODEL AS907 TURBOFAN ENGINE

During the engine fan blade-out containment test, a fan blade was intentionally released by artificial means while the engine continued to operate for 15 seconds after the event. The engine was then shutdown by the operator. The released blade penetrated the containment system, but stopped between the fan housing and the fabric wraps. Figure 3-3 shows a still frame photograph of particular interest from the high-speed motion picture taken during the test in which just the tip of the intentionally released fan blade is shown sticking out of the last fabric layer. Figure 3-4 shows photographs of the disassembled fan housing immediately after the test with the intentionally released blade at its resting position. The airfoil had penetrated the containment system up to approximately mid span, but the heavier root section, including the platform and the shank, was contained within the fabric wraps. The blade tip was damaged and bent due to the resulting impact. Although this containment test stopped the blade, the design was modified for certification test by increasing the number of layers by approximately 15 percent to achieve additional safety margin. As a result, during the official AS907 certification test, the intentionally separated fan blade was entirely contained within the fabric containment system.

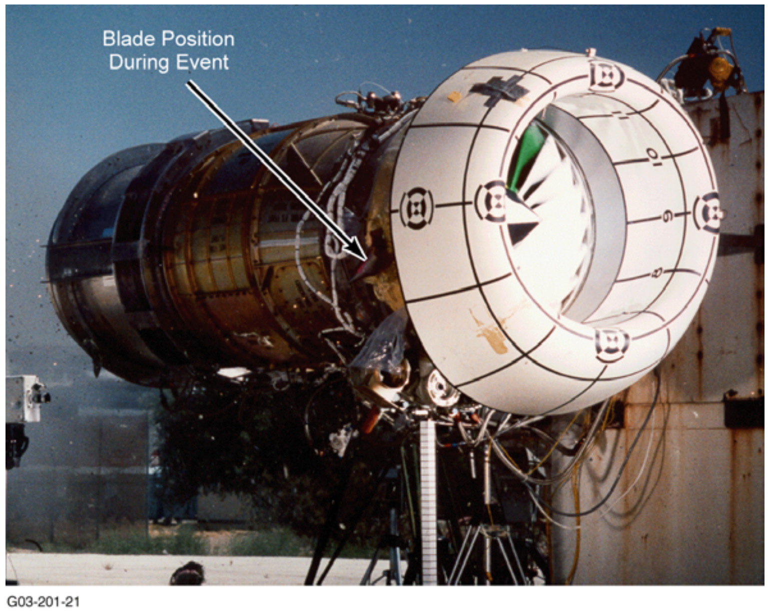

FIGURE 3-3. FRAME FROM A HIGH-SPEED MOVIE OF THE AS907 FAN BLADE-OUT TEST

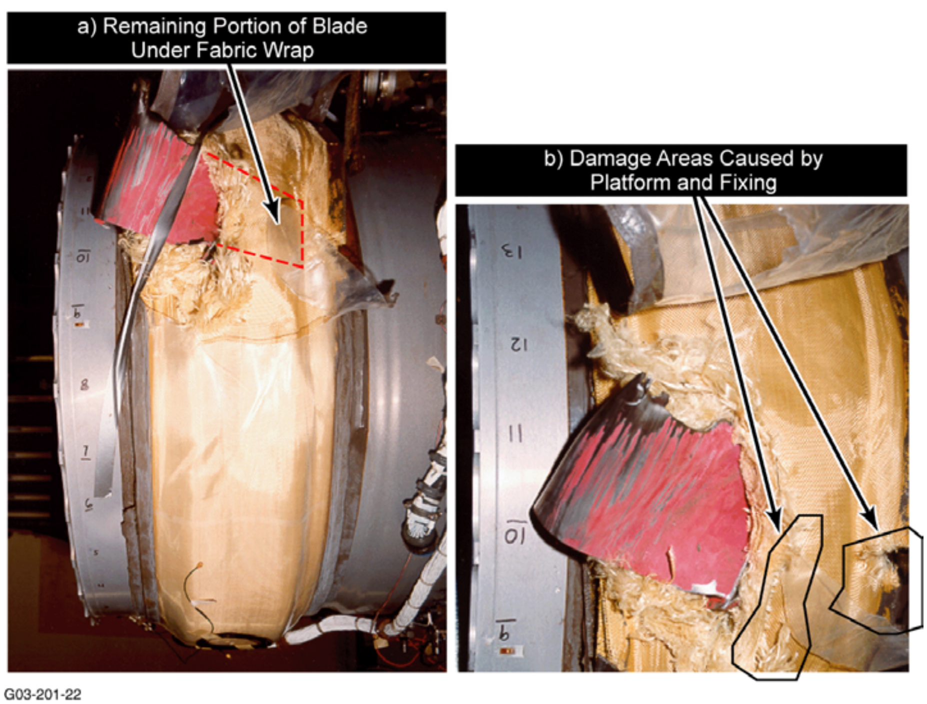

FIGURE 3-4. AS907 FAN CONTAINMENT HOUSING FOLLOWING BLADE-OUT TEST

3.4 ANALYSIS RESULTS.

3.4.1 Baseline (1999) Analysis.

During design, before execution of the above engine test, an LS-DYNA analysis was conducted to guide the containment design incorporated into the test engine and also to predict the possible outcome of the test. The objective of the analysis was not only to predict the containment capability of the composite fabric system but also to predict the performance of other design features contributing to the success of such complex designs. Therefore, this analytical model not only included the containment hardware but also a good portion of the front section of the engine to study blade-to-blade interactions, shaft dynamic motion and interaction with support structures, and the dynamic loads transmitted to the remaining structures and to the engine mounts, etc. As a result, as shown in figure 3-5, this model was very large and cumbersome to use in the present fabric containment study. A subportion of the model was extracted to simulate blade release and the containment event only, as also shown in figure 3-5. This reduced model was already confirmed in 1999 to have adequately captured the physics and boundary conditions of the full model for the containment portion of the problem. The reduced model includes two blades (one released and one trailing) and the fan containment hardware, with three shell layers representing all the fabric layers as well as other layers, such as the metallic housing, abradable coating, and honeycomb and graphite epoxy shell.

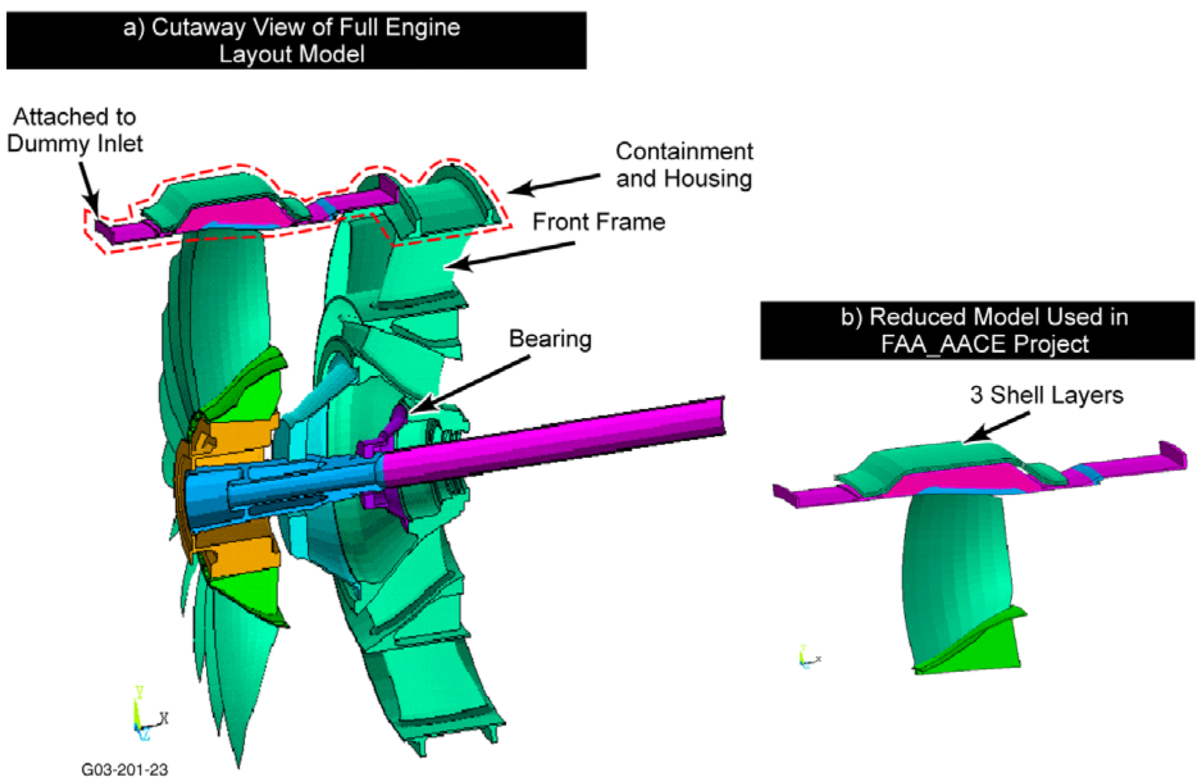

FIGURE 3-5. LS-DYNA MODEL FOR FAN BLADE-OUT CONTAINMENT ANALYSIS

To establish a proper baseline, the 1999 fan blade containment analysis was repeated again with the current version of the program and current computer hardware. The result is qualitatively presented in figure 3-6, where the picture shows the final condition of the hardware when the containment event was over (5 milliseconds after blade release). When compared to actual posttest engine hardware photographs, the predictions were found to be on the optimistic side. The fabric layers were not perforated and the containment system did not show any signs of distress. Also, the blade deformation during the impact did not correlate well with the posttest hardware observations.

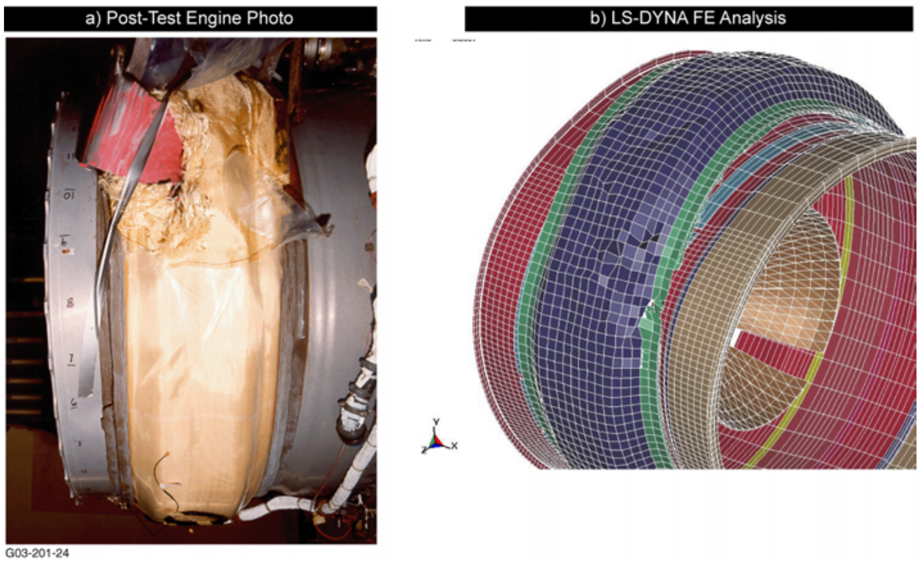

FIGURE 3-6. 1999 BASELINE FAN CONTAINMENT ANALYSIS—OVERALL VIEW

The following specific features of this model should be noted:

- The mesh density of the fabric layers was considerably coarser than the ballistic model mesh density, namely ~0.750 inch (19 mm) compared to 0.250 inch (6.4 mm).

- Three shell-element layers were used to represent all the fabric layers. This configuration worked well within LS-DYNA, without any contact-related instabilities. The coarse mesh density might have helped for the possible contact issues.

- Kevlar was modeled with a standard elastic-plastic material model, which is mainly used for metallic materials. This is a very rough assumption because the composite fabrics do not behave like metallic materials.

- The physical fabric thickness was used as the basis for the shell elements representing the fabric. This is not exactly correct, for reasons discussed in section 2.3.

- The fan blade was modeled with coarse shell elements. It should be noted that the projectile in the earlier ballistic test simulation was modeled with solid elements with a fine mesh density.

Nevertheless, except for the optimistic fabric behavior and the unrealistic blade deformation, the other aspects of the containment event were simulated quite well. Figure 3-7 compares the results of the baseline analysis against actual hardware damage in terms of the blade-housing interaction, blade final orientation within the sacrificial containment hardware, and secondary damage created by the blade.

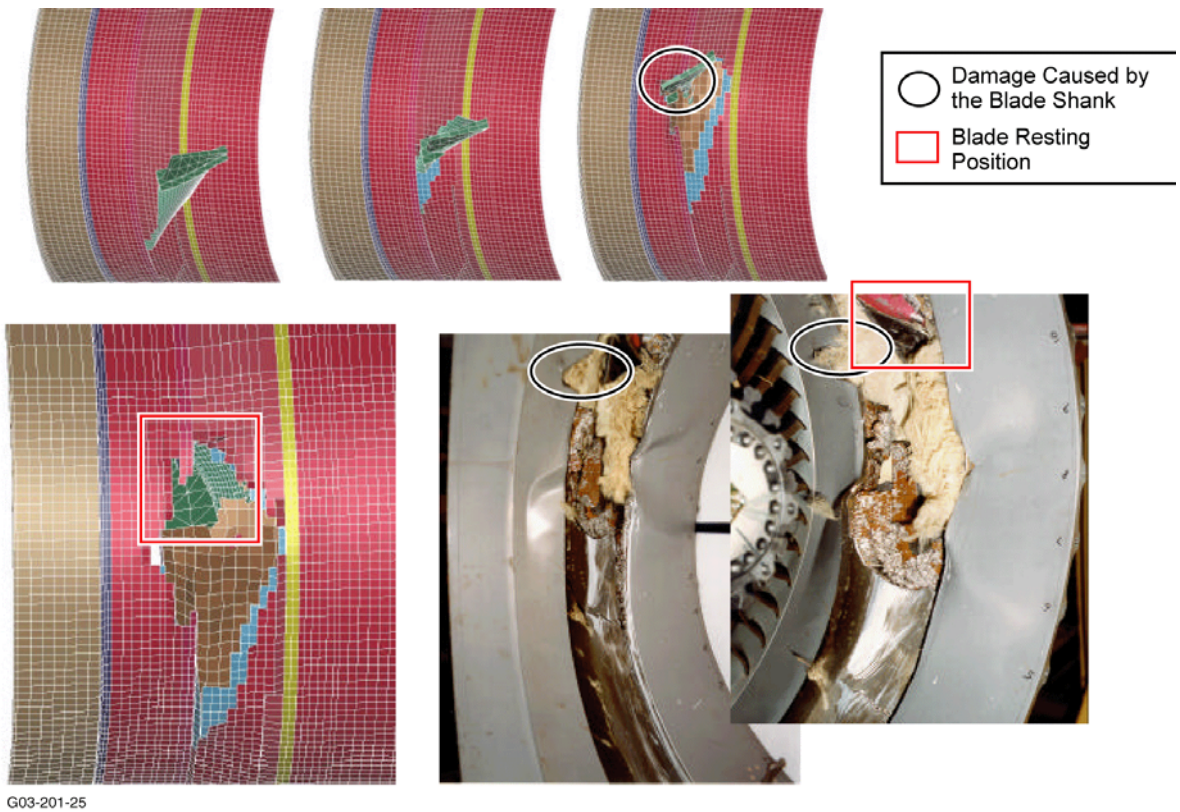

FIGURE 3-7. 1999 LS-DYNA BASELINE FAN CONTAINMENT ANALYSIS—PREDICTED INTERNAL DAMAGE

3.4.2 1999 Model With New Kevlar Material Formulation.

In the next step of the investigation, the baseline 1999 analysis was repeated, but this time the fabric material model developed during this research program was introduced to replace the 1999 material model. As discussed in section 2, this material model was used and calibrated with the equivalent half-thickness concept; therefore, the fabric shell thicknesses were also updated for consistency. Other features such as fabric mesh density, shell blade elements, number of shell layers modeled (three), and legacy contact types were not modified. Figure 3-8 summarizes the results with the isolated effect of the material model and compares the resulting predicted hardware damage to the actual engine test results. Incorporation of this new material model had a large effect on the overall outcome, when compared with the results from the baseline analysis. The blade was estimated to completely rip the fabric layers, making the prediction more conservative with respect to the actual test. It is also worth noting that the multishell modeling (three shell-element layers) was still successful.

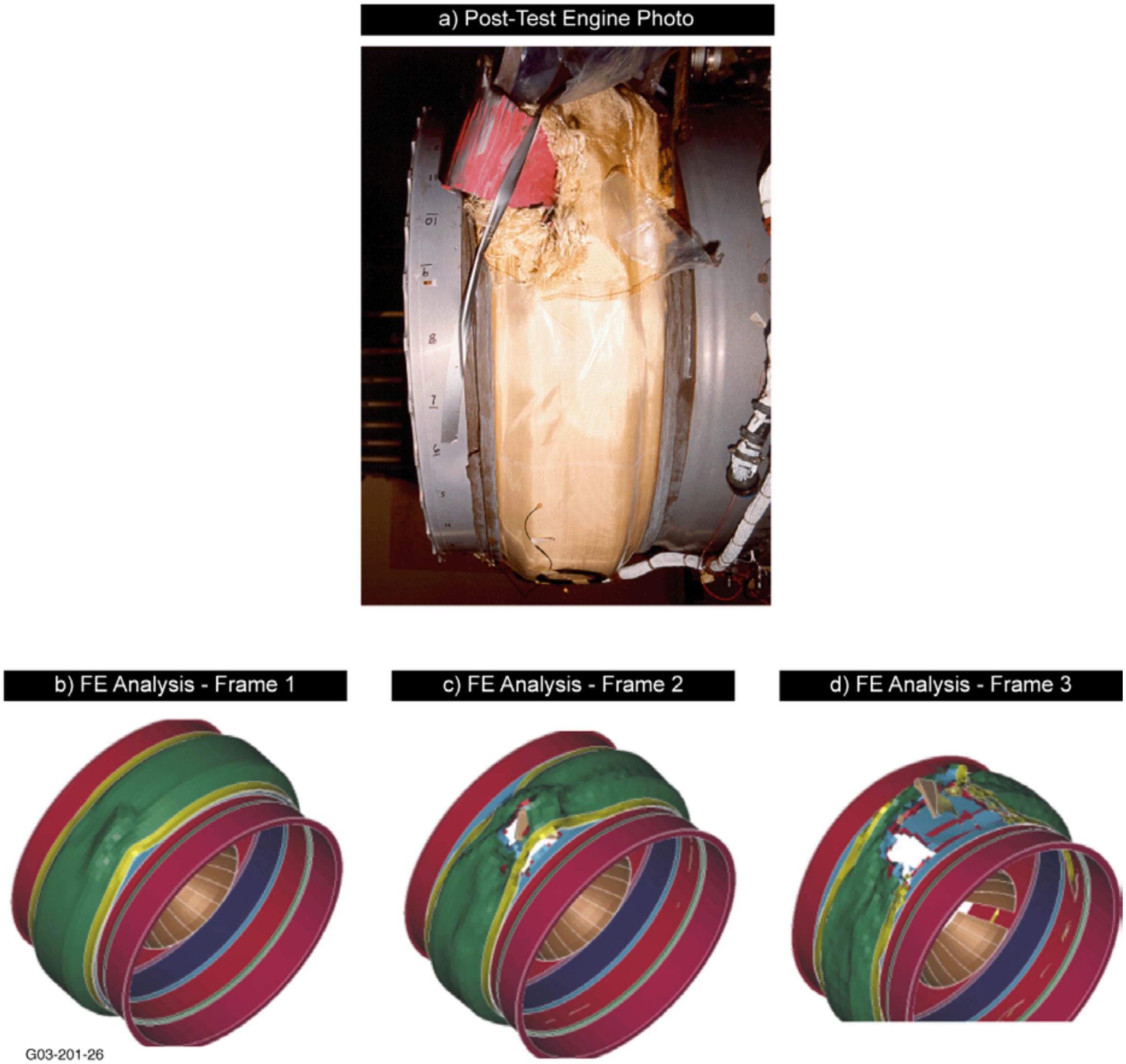

FIGURE 3-8. 1999 LS-DYNA MODEL ENHANCED WITH NEW KEVLAR MATERIAL FORMULATION

3.4.3 Optimized Methodology and New Kevlar Model.

In the final phase of the engine fan blade-out simulations, other modeling techniques developed in the earlier calibration work were also introduced in the analysis in addition to the new material model. The LS-DYNA model was modified to incorporate a single-layer shell representing all fabric wraps, since this method was shown to be the most consistent during the earlier ballistic simulation work. The mesh density was also refined to be consistent with the ballistic test simulation models. The blade was also modeled more realistically using solid elements. Finally, the new advanced contact types (SOFT=2), which gave the best results during the ballistic test simulations, were also incorporated into the analysis. As shown in figure 3-9, the predictions matched much better with the overall behavior seen in the engine test.

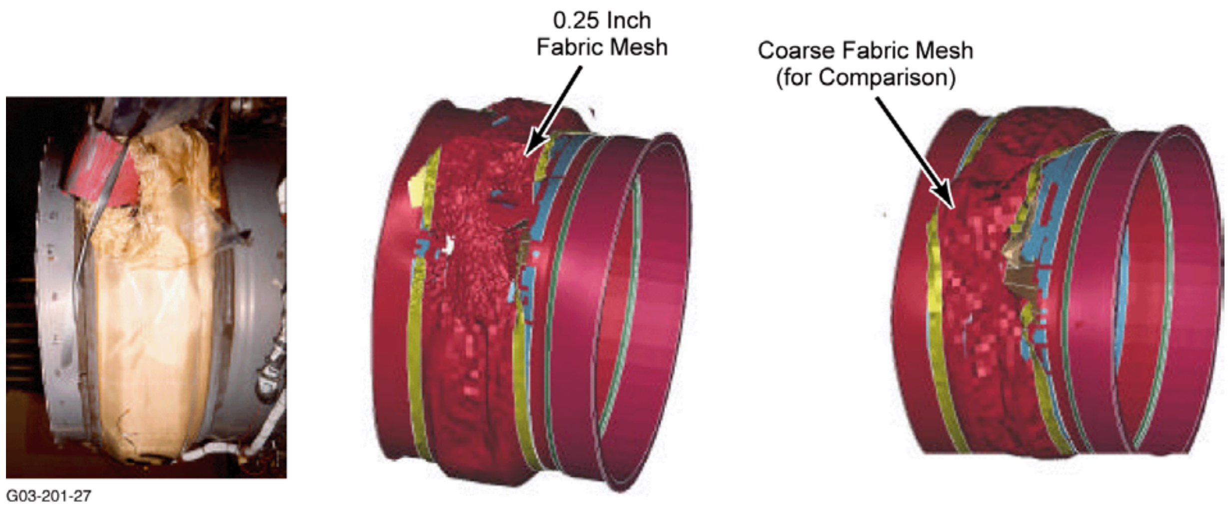

FIGURE 3-9. LS-DYNA ANALYSIS WITH OPTIMIZED METHODOLOGY
AND NEW KEVLAR MODEL

It was predicted that the fabric layers would be punctured by the blade tip at the front portion of the containment system and that the blade tip would also be exposed, as it was in the engine test. The damage caused by the heavy root portion of the blade at the aft section of the fabric system was also realistically captured. Predictions obtained with a coarser fabric mesh density similar to the 1999 model are also shown in figure 3-9. Comparison of the predictions with the two mesh densities suggests that the coarser mesh model produces more optimistic results. This is also consistent with the results of the 1999 analysis. Predicted damage to the internal (nonfabric) components of the containment system is shown in figure 3-10. The extent of damage made by the blade, the size of the opening before reaching the fabric layers, and the location of the impact of the heavy blade shank with the housing wall were realistically captured. Similarly, the deformed posttest shape of the blade was successfully predicted, including features such as the tip section curved opposite to the direction of rotation, the tip leading edge and the shank trailing edge severely damaged, and the platform severed by the impact of the trailing blade. This type of detailed information permits the containment designer to consider other aspects of the fan containment problem, such as support structure integrity, and blade design.

An attempt was made to replace the single-layer fabric model in figure 3-10 with a three-layer model to duplicate the results. This could not be achieved because of premature analysis termination due to extensive element distortion and contact instabilities. The software program manufacturer was consulted in an attempt to resolve these issues, but these efforts were unsuccessful. The reasons for failure of the multilayer modeling capability compared to the earlier successful ballistic test simulations and the 1999 modeling are not well understood. It is speculated that the very fine mesh density used in this complicated model could have negative effects. No further work was performed to investigate this effect.

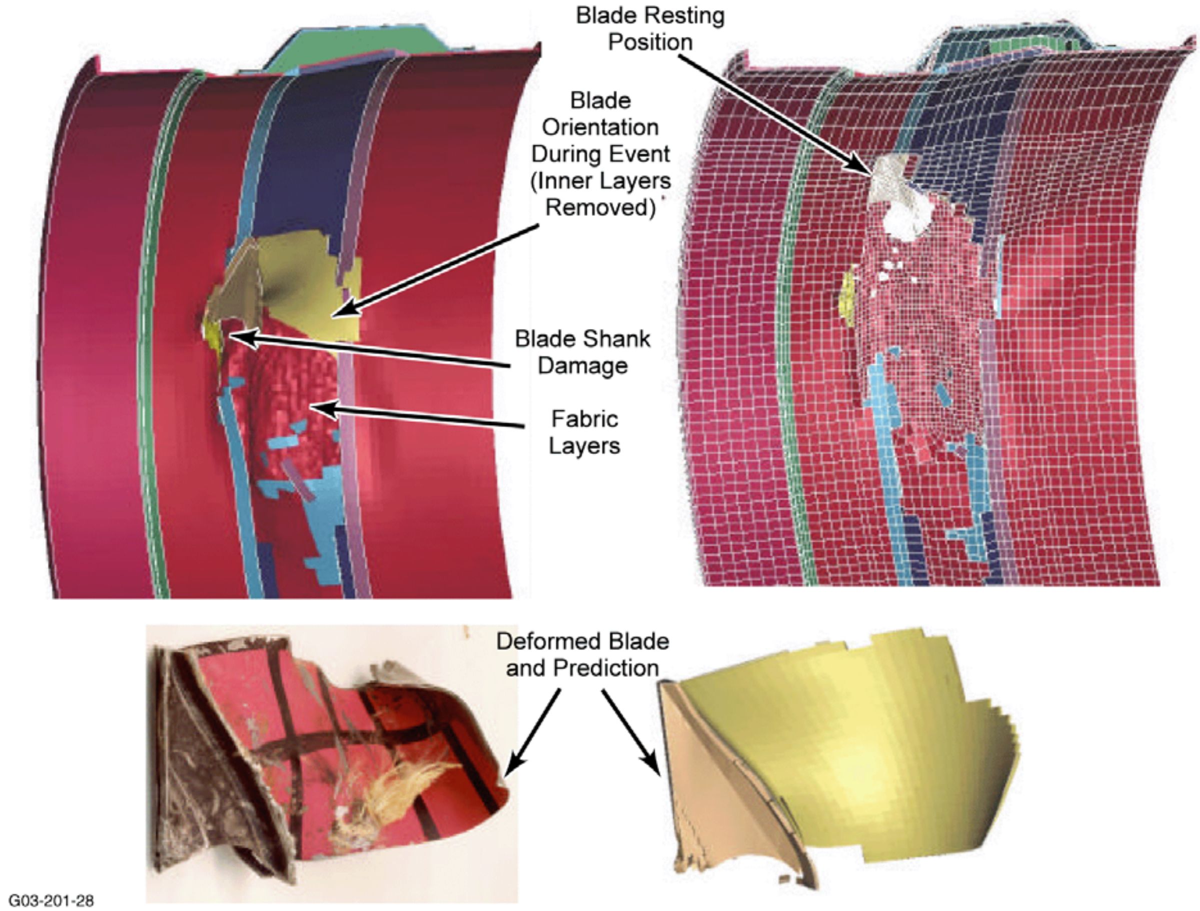

FIGURE 3-10. LS-DYNA ANALYSIS WITH OPTIMIZED METHODOLOGY AND NEW KEVLAR MODEL—PREDICTED INTERNAL DAMAGE

As already discussed in section 3.3, although the containment system stopped the blade during the AS907 engine development test, the design was later modified for the upcoming official certification test by increasing the number of layers by approximately 15 percent for additional safety margin. As a result, during the AS907 fan blade-out certification test, the intentionally separated blade was entirely contained within the fabric system. An updated analysis with the AS907 design changes incorporated was also performed with LS-DYNA, and the new results correlated well with the final engine qualification test results.

3.4.4 Fan Containment Predictions With Zylon.

To study differences in behavior between Kevlar and Zylon materials in a fan containment environment, the Kevlar material properties used in section 3.4.3 were replaced by properties for Zylon material. However, there were no fan blade-out containment test results using Zylon to make a thorough comparison. Nevertheless, the analytical comparison results using Zylon have great value in determining the ability of the analysis to reflect the conclusions drawn from the ballistic tests (i.e., Zylon has equal or slightly better capabilities) in a more complex containment environment. No other geometrical changes were made in the model, and the number of layers simulated was kept the same, except the total thickness of the Zylon fabric wraps was properly simulated. Comparison of the Zylon and Kevlar analysis results shown in figure 3-11 indicates that a similar containment capability (based on the total amount of energy absorbed) is predicted when Zylon is substituted. In general, a similar level of containment was predicted with both materials in terms of retaining the separated blade within the containment system; whereas some details were observed to be different. For example, in a manner consistent with the ballistic test results, the slightly higher properties of Zylon prevented local penetration of the separated blade. But at the same time, higher hoop loads developed within the fabric layers, causing more axial ripping of the layers, without total release of the blade. It should be noted that even if the containment capability of Kevlar and Zylon is the same for this design (considering a similar number of fabric layers for both materials), Zylon offers a substantial weight reduction because of its 30 percent lower density when comparing the Kevlar 49 (1490 Denier, 17 × 17 mesh) to the Zylon (500 Denier, 35 × 35 mesh) used in the analysis.

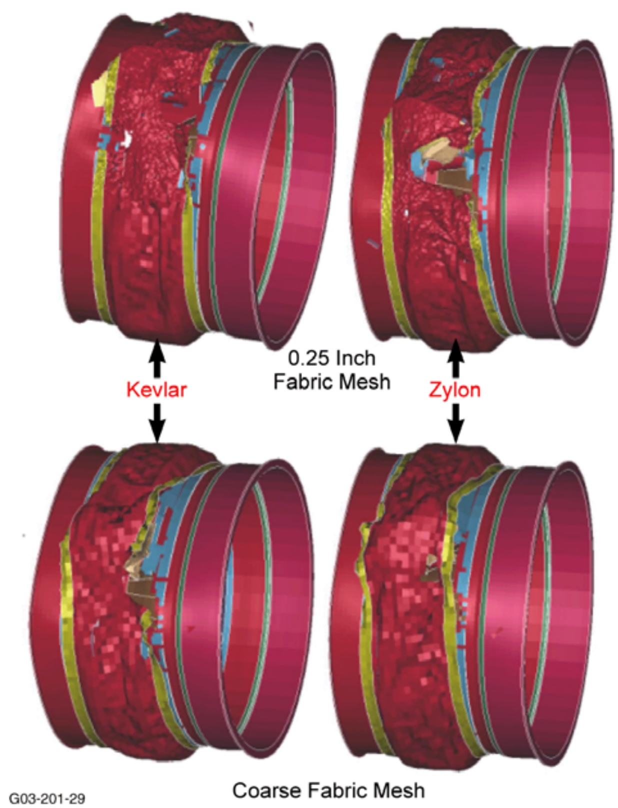

FIGURE 3-11. LS-DYNA PREDICTIONS WITH KEVLAR AND ZYLON MATERIAL

3.5 CONCLUSIONS.

The conclusions drawn from the task 4 results are summarized as follows:

- An engine fan blade-out event was successfully simulated using the fabric material models and developed analytical methodologies.

- Acceptable correlation was obtained between the simulation results and the engine containment test results, using the new Kevlar material model and the single shell-layer modeling technique.

- Prediction capability was significantly improved with the new material model and the associated modeling techniques, with respect to the previously used (1999) methodology.

- In spite of successful results during the ballistic test simulations, further analytical enhancement with multilayer modeling was not possible, due to numerical instabilities.

- Comparison of Kevlar and Zylon capabilities within the same containment design revealed containment results consistent with the ballistic test results trends. For the same number of fabric layers, Zylon offers weight reduction possibility if it is used in lieu of Kevlar.

- The mesh density was kept constant during the program, but the possible effects on the results were not investigated. Further investigation of the effects of mesh sensitivity, contact parameters, and multilayer numerical instabilities are recommended.

4. GENERIC CONTAINMENT MODEL.

4.1 OBJECTIVE.

One of the deliverables of this research project was to build and provide a Generic Containment Finite Element Model for Kevlar or Zylon wrap materials. The purpose of this model was to provide LS-DYNA users with generic guidelines for modeling composite fabric wraps in impact containment-related applications.

4.2 BACKGROUND.

During the planning stage of this project, specifics of the generic model were not defined but were left to the participants of the project, depending upon the outcome of the previous tasks. One possibility considered was to build a model of a simplified engine containment system, including fabric layers, a metallic support housing, and a generic blade as the projectile. After completion of task 4, it was concluded that this type of problem was too complex for the purpose of initiating typical LS-DYNA users to fabric-related impact simulations. Another downfall of a fictitious engine containment model was a lack of experimental test data to verify the accuracy of predictions that potential users may obtain by experimenting with various parameters.

Therefore, it was decided, in principle, to provide a complete tool, including the numerical model and the test results, which will give users the possibility to study and calibrate their own analytical systems. The only comprehensive fabric experimental test data available to date that can be used to support analytical predictions is the ballistic tests performed by NASA GRC under this research program. Therefore, it was decided to electronically provide the LS-DYNA finite element models (refer to section 2.3) to satisfy the requirements of the Generic Containment Model. Potential users will be able to run these models, which are already set up with appropriate materials, contact algorithms, boundary conditions, etc., with their respective software versions, operating systems, and computer platforms, to observe any variations with respect to the results already reported herein. Section 6 gives a brief discussion of the variations in the results that can be experienced using LS-DYNA, depending on the contact types, processor types, and computer platforms. This discussion, together with the ballistic test simulation model, will guide the users to experiment with the simulations, keeping always in sight the corresponding experimental results.

4.3 GENERIC MODEL FILES.

The computer files constituting the generic containment model are included in the CD-ROM version of this report. A list of the files and their descriptions is given below:

a. zylon_1x4.input: This is the complete LS-DYNA input deck, including the following:

- Baseline LS-DYNA control cards used in the current study.

- Finite element nodes and elements simulating the four-layer Zylon ballistic test. One layer of shell elements was modeled to simulate four layers of fabric (1x4).

- User material input for Zylon (see appendix A) compatible with the developed fabric material model. Kevlar material input is also included. The user can convert this model to an alternative model for Kevlar simulations by switching to the Kevlar properties instead of Zylon (shell thickness should then be updated accordingly). The material properties for the steel components are also provided in the input file.

- Shell thickness definition for four-layer Zylon. For Kevlar analyses, change the thickness to the appropriate four-layer Kevlar thickness.

- Definition of parts within the model.

- Contact types (cards) between defined parts.

b. zylon_1x4.results: This is the directory containing the output files of the analysis performed using zylon_1x4.input. These results were obtained using the following:

- LS-DYNA code (before the user-defined material compilation): ls960_s_447_hp_102

- LS-DYNA version 960, revision 477

- HP8000 Unix machines, with operating system version 10.2, single processor, and single precision.

c. ansys_model_1x4.db: This is the ANSYS model defining the geometric configuration of the ballistic test (single shell model). Geometry is available for further modifications to zylon_1x4.input, if desired. This also includes bare finite element model (nodes and elements) but not the control cards, contact cards, and part definitions. This model is required if other thicknesses for the shell elements (rather than the thickness provided above) are investigated. For example, for a desired 1x8 model, the total thickness of the shell can be easily modified in the input file, but the shell (fabric) mid-plane should be adjusted using this model file to provide the required gap between the shell surface and the support ring.

d. zylon_4x1.input: This is the complete LS-DYNA input deck, similar to zylon_1x4.input, except the following:

- Finite element nodes and elements simulating the four-layer Zylon ballistic test. Four layers of shell elements were modeled to simulate four layers of fabric (one fabric layer per shell, 4x1).

- Shell thickness definition for one-layer Zylon, since all layers are explicitly modeled. For Kevlar analyses, change the thickness to appropriate single-layer Kevlar thickness.

e. zylon_4x1.results: This is the directory containing the output files of the analysis performed using zylon_4x1.input.

f. ansys_model_4x1.db: This is the ANSYS model defining the geometric configuration of the ballistic test (multiple shell model). Geometry is available for further modifications to zylon_4x1.input, if desired. This also includes bare finite element model (nodes and elements) but not the control cards, contact cards, and part definitions. This model is required if more shell layers are to be considered. For example, for a desired 8x1 model, this model can be modified to create extra shell layers. Depending on the number of fabric layers that each shell layer represents (8x1 or 4x2), the thicknesses and the shell-to-shell or shell-to-ring gaps should be adjusted.

g. fabric_material_code: This is the user-defined FORTRAN code defining the composite fabric (Zylon and Kevlar) material behavior. This file should be used in conjunction with the baseline LS-DYNA binary files to create a user-defined LS-DYNA executable. This file has been successfully used on the HP8000 Unix machines. For other platforms, changes to the FORTRAN program might be required to make it compatible with the specific compiler.

h. read_me.txt: This file provides descriptions of the above files as well as the lessons learned that are discussed in the following section.

4.4 GENERAL MODEL RECOMMENDATIONS.

The following recommendations provide the potential users of the Generic Containment Model with important tips about its capability and limitations. The lessons learned, obtained during the course of the project, are also included.

a. The first thing that the user should do is to choose the appropriate version of LS-DYNA to compile the user-defined material model. The binary models can be downloaded from a special FTP website maintained by the LS-DYNA supplier, Livermore Software Technology Corporation (LSTC). Not all of the LS-DYNA versions and revisions for different operating systems and platforms have a user-defined material capability. Please note that the example problems and the results were obtained with a specific computer setup, as noted in section 2.4.

b. Next, the user should establish a baseline capability of the LS-DYNA version on the computer hardware available. If more than one computer platform is available to the user, it is strongly recommended to compare the results from one of the examples given, using each of the platforms. The results might be different, especially if the same problem is analyzed using single processing or massive parallel processing.

c. For a given computer platform, the largest source of variation in the results is due to the various contact algorithms available in LS-DYNA. The user should read the parametric study discussed in section 6 to learn more about the effects of the contact parameters.

d. The same contact type and parameters were consistently used in all the simulation analyses as reported in the previous sections. Particularly in the fabric containment problem where a stiff projectile hit a low stiffness fabric, the successful contact parameters are hard to pick. Throughout the analyses of the current research, segment-based SOFT=2 (automatic surface-to-surface contact type) was consistently used. Although other types of contact algorithms were initially considered, the best results for the simulation of the fabric impact problem were obtained by using this contact type. The SOFT=2 option causes the contact stiffness to be determined based on stability considerations, taking into account the time-step and nodal masses. This approach is generally more effective for contact between materials of dissimilar stiffness or dissimilar mesh densities. The best results were also obtained by using slave and master contact penalty factor (SFS and SFM) of 0.1.

e. Another parameter that is closely related to the successful contact modeling is the time-step. With the contact setup of item d, a reduced time-step was concluded to give the most stable solution to the expense of longer computational time. The time-step scale factor TSSFAC in the *CONTROL_TIMESTEP control card was, therefore, set to 0.2.

5. JOHNSON-COOK MATERIAL MODEL.

5.1 BACKGROUND.

An additional investigation was done to compare the performance during impact analyses of the Johnson-Cook material model recently improved by LLNL and the conventional Honeywell metallic material model. The Johnson-Cook material model is specific to metallic materials used in impact applications. The containment system of the Honeywell engine described in section 3.3 is conceptually a fabric wrap system, and the contribution of the metallic support layers are negligible. This system is, therefore, not adequate to investigate the performance of a material model designed for metallic materials. Since LLNL had already modeled a published impact test using its material formulation and obtained successful results, it was decided to use the same analytical model to obtain comparative results using the alternative Honeywell material model.

5.2 JOHNSON-COOK MATERIAL MODEL BY LLNL.

Several material models have been developed which can represent, with varying degrees of accuracy, the high-strain rate deformation response of materials to adequately formulate the penetration and perforation of aircraft and engine materials. Of these, the Johnson-Cook model, which was developed during the 1980s to study impact, ballistic penetration, and explosive detonation problems, is the most widely used, and it has been introduced in explicit finite element codes such as DYNA-3D and LS-DYNA. Its use for a particular material, however, requires determination of many material constants and also failure strain damage parameters. A LLNL report [3] describes the motivation for using the Johnson-Cook material model in simulations involving engine containment and engine debris mitigation on aircraft structures. In that report, experimental studies of the deformation and failure behavior of Ti-6Al-4V and 2024-T3 aluminum at high strain rates and large strains were reported. The report also describes the generation of material constants for the Johnson-Cook strength model. A more recent report [4] describes the determination and validation of parameters for Ti-6Al-4V and 2024-T3 aluminum that can be used in the failure portion of the Johnson-Cook material model. The governing equations representing the material behavior and the failure strain damage accumulation can also be found in the same references.

5.2.1 Impact Analysis Using the Johnson-Cook Material Model.

The flow surface material constants and the failure parameters that were obtained by the Hopkinson bar test simulations are given in table 5-1 [3 and 4].

TABLE 5-1. JOHNSON-COOK MATERIAL CONSTANTS FOR Ti-6Al-4V DETERMINED BY LLNL

Yield Surface Parameters				
A	B	C	n	m
159.2 ksi	158.4 ksi	0.014	0.93	0.11
Failure Strain Parameters				
D_1	D_2	D_3	D_4	D_5
-0.090	0.270	0.480	0.014	3.870

The failure strain parameters were validated by LLNL using DYNA-3D on penetration test data, as shown in figure 5-1 (reproduced from reference 4). The report [4] states that the test targets were rolled plate Ti-6Al-4V, per specification Aerospace Material Specification (AMS) 4911, 0.601 inch (15.3 mm) thick. The targets were in a free-boundary condition, hanging from holes in the corner of each 36-inch- (914-mm)-square flat plate. The projectiles weighed approximately 8 lbs (3.6 kg) and were beveled at the nose to simulate a fan blade root impact footprint. The finite element model solution convergence issues were simplified in this study by maintaining close to uniform mesh resolution for the Ti-6Al-4V simulations. The through-the-thickness mesh resolution of this three-dimensional, 1/4 symmetry model was 0.05 inch (1.3 mm) per element. An element aspect ratio less than 3:1 was maintained throughout this portion of the study. Eight-node solid brick elements with a one point integration were employed throughout this study. The outer regions of the targets were sometimes meshed with fewer elements through the thickness (by a factor of three) and then tied to the finer-zoned impact region to reduce the number of elements in each calculation. The finer-zoned impact region extended to between two to three times the relevant impactor dimension.

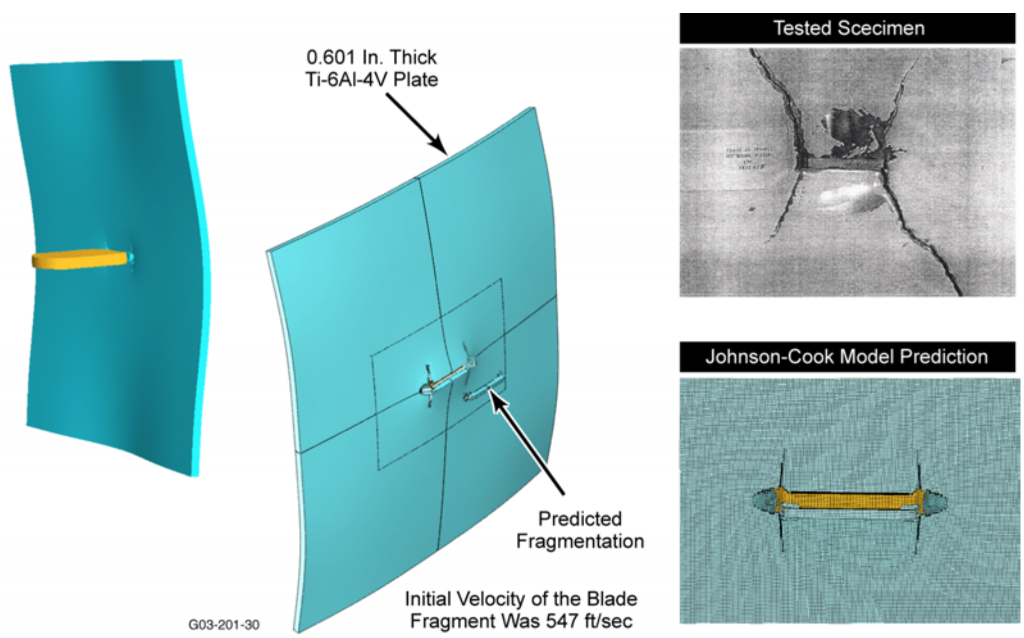

FIGURE 5-1. THE LLNL ANALYSIS USING THE JOHNSON-COOK MATERIAL MODEL

The available test data consisted of the initial conditions plus photographs and observations of the posttest target condition. The simulation predicted the correct amount of penetration and approximate crack patterns.

5.2.2 Impact Analysis Using the Honeywell Material Model.

Before performing any comparison work with an alternative material model, Honeywell reran the same analysis using computer platforms and LS-DYNA versions consistent with other work reported in this document. The LLNL DYNA-3D finite element model was converted to an LS-DYNA model by LLNL and provided to Honeywell. The material constants listed in table 5-1 were used to activate the LS-DYNA-embedded material model, *MAT_JOHNSON_COOK (material type 15). After a baseline was established, the material model was replaced with the elastoplastic material model widely used in impact applications at Honeywell. This later model does not have the capability to represent material behavior under high strain rates, but it is used in a variety of applications because of its simplicity (no material constants). Figure 5-2 shows the comparison between the results produced by the two material models. Except for deflections at the outside boundaries of the plate, the baseline analysis using the Johnson-Cook model produced very similar results to figure 5-1.

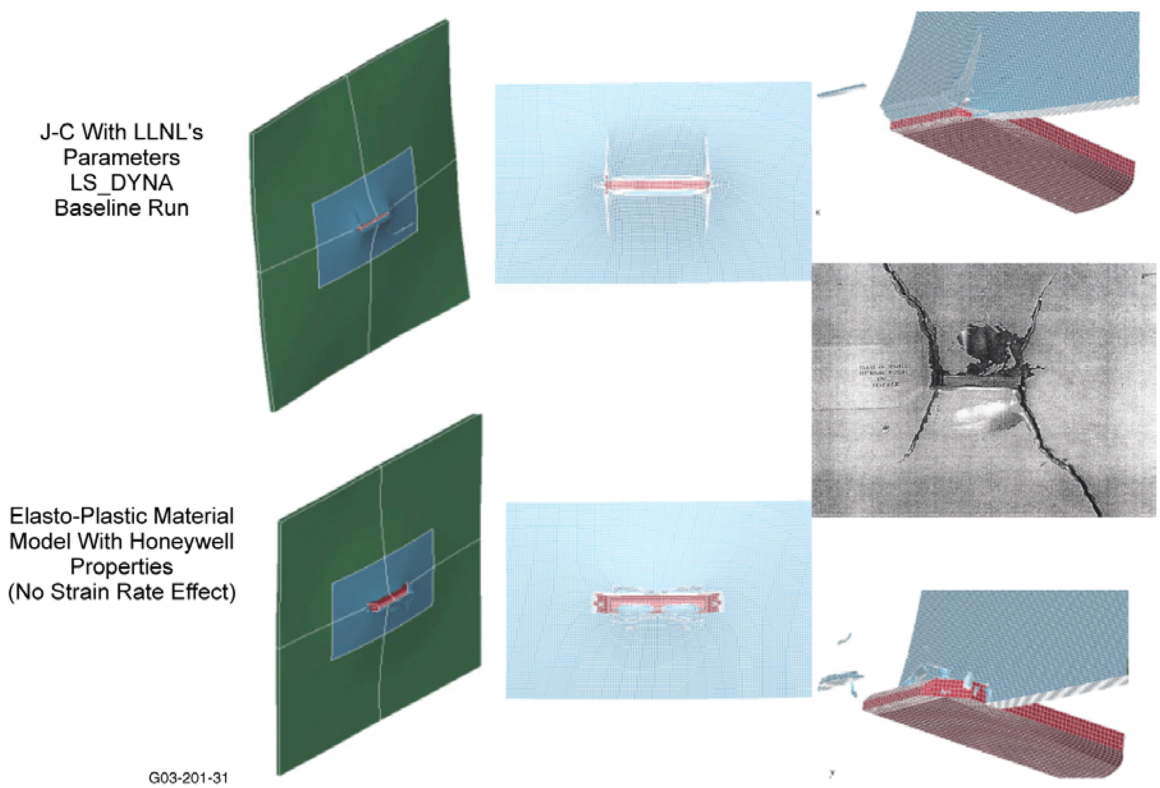

FIGURE 5-2. COMPARISON OF PREDICTIONS USING THE JOHNSON-COOK AND ELASTOPLASTIC MATERIAL MODELS

On the other hand, for the example investigated, the conventional Honeywell material model could not adequately represent the test results. The simulation could not predict the petalling type of failure of the target, nor the crack patterns from the corners. Rather, the analysis predicted a shear (plug) type of failure for the plate.

5.3 CONCLUSIONS.

The conclusions drawn from the Johnson-Cook material model comparison results are summarized as follows:

- The Johnson-Cook material model provided a more realistic simulation of the test results than the alternative model.

- The predicted failure modes were different for the two material models investigated. The Johnson-Cook model predicted a petalling type of failure, whereas the alternative model indicated a shear failure.

- The Johnson-Cook model successfully predicted the complete energy absorption of the test, whereas the elastoplastic model conservatively predicted only 85 percent.

- The Johnson-Cook model requires an extensive evaluation of the set of material constants for every material involved in a given practical problem. The alternative method is noted to be simple and inexpensive.

- A very high mesh density was absolutely required to accurately simulate the test results with the Johnson-Cook model in the simple example studied: 1/4 model; 4 × 110,000 elements. In a typical engine containment model, it is not practical to use this type of mesh density, i.e., the task 4 fan blade-out containment problem featured approximately 30,000 elements.

6. ISSUES, LIMITATIONS, AND LESSONS LEARNED.

6.1 BACKGROUND.

The LS-DYNA explicit finite element program is considered to be an excellent design tool to address impact and penetration modeling problems. The popularity of LS-DYNA is continuously increasing, especially in dealing with complex aerospace applications such as rotor fragment containment. For example, at Honeywell, LS-DYNA has permitted the successful design and optimization of a variety of gas turbine engine containment systems. Using LS-DYNA has been instrumental in considerably reducing the number of expensive tests required to validate such containment designs. On the other hand, adaptation of LS-DYNA to impact-related problems is not straightforward and requires careful understanding of the effects of the parameters involved. Users should understand that, as in any other complex analysis tools, a certain variation in results exists in LS-DYNA analyses. It is the user's responsibility to understand the effects of the control parameters and to use them to adequately represent the physical behavior studied.

In the following sections, variations in the results encountered during the course of the project, due to some computer hardware or software environments and due to contact choices dealing with part-to-part interaction, are summarized. The purpose of including this material is not to provide an absolute answer as to how to set these parameters but to promote better user awareness about possible variations when using LS-DYNA.

6.2 EFFECTS OF COMPUTER PLATFORM AND SOFTWARE VERSION/REVISION.

In the course of the ballistic test simulations of composite fabric systems (see section 2), it was observed that conducting the same analyses at SRI and Honeywell gave different results, in terms of how much of the fragment kinetic energy was absorbed by the barrier. LSTC was contacted to isolate the reason for these differences, including the fact that analyses at Honeywell and SRI were performed on different platforms, using different versions or revisions of LS-DYNA. To avoid the possible effects of the newly created material model for fabrics, it was decided to create a more conventional impact example to investigate platform and revision issues.

For this investigation, a simpler model was analyzed using standard material models in LS-DYNA rather than the material model being developed by SRI for fabrics. This model consisted of a 0.160-inch- (4.1-mm)-thick steel plate impacted by a steel projectile. The kinetic energy absorbed by the barrier is calculated as the difference between the initial and residual kinetic energy of the projectile. A summary of the results of the calculations on different platforms and with different slideline types and parameters are listed in table 6-1. Because this case uses steel properties for the barrier, there are no experimental results to compare the analyses against.

TABLE 6-1. LS-DYNA PLATFORM, VERSION/REVISION INVESTIGATION SUMMARY

Platform	Version/Revision	Percent Kinetic Energy Absorbed				
		LS-DYNA Contact Type				
		Auto Surface to Surface			Single Surface	
		Soft=0	Soft=1	Soft=2	Auto	Erode
HP	ls960_s_447_hp8000_102	27.3	28.5	39.9	25.1	26.7
IBM	ls960_s_447_ibmpwr3_43_p	27.0	28.5	39.9	26.1	26.7
IBM	ls960_d_447_ibmpwr3_43_p	27.0	30.5	39.8	25.9	26.8
HP	ls960_s_1488_hp8000_102	27.3	27.8	39.9	25.7	27.1
IBM	ls960_s_1488_ibmpwr3q32_43_p	27.0	28.1	39.9	25.7	27.0
IBM	ls960_d_1488_ibmpw3_43_p	27.2	30.2	39.9	25.8	27.0
Linux	ls960_s_1488_linux_71_p	25.2	30.2	---	24.1	---
Linux	ls960MPP_s_3041_linux_lam652pg	24.0	29.4	46.1	25.0	23.9

Example:	ls960_d_447_ibmpwr3_43_p Ls960: version d: double precision (s: single precision) 447: revision ibmpwr3: computer platform 43: operating system version p: parallel processing

Honeywell used Hewlett-Packard (HP) and International Business Machines (IBM) Unix workstations, whereas SRI used PC-based Linux clusters. The Linux-based system was capable of multiparallel processing. The findings are summarized as follows:

- The LS-DYNA results are consistent across computer platforms, given the same input and the same code version/revision.

- Different versions of LS-DYNA will give different results with the same input, although the differences are not very large. Between Unix machines, differences were a maximum of 5 percent, regardless of the revision, precision, or the operating system used. The largest difference observed was between the Unix and Linux machines, up to 16 percent.

- Based on further investigations, it was found that the differences in results depended upon the complexity of analyzed problem and how intense the nonlinear contact/failure mechanisms were. For example, a subsequent analysis using one of the ballistic fabric analyses contained in section 2 showed that the results could be as much as 20 percent different between IBM and HP machines.

- Different contact formulations will give significantly different results for the same problem (using the same version and platform). Further investigation was performed and is reported in section 6.3.

6.3 EFFECTS OF CONTACT PARAMETERS.

Some of the contact parameters of LS-DYNA were varied on the same example to find out the variation in the results. The computer platform and the program version were kept the same. Figure 6-1 summarizes the findings. Automatic-single-surface, eroding-single-surface, surface-to-surface, and automatic-surface-to-surface are standard contact options within LS-DYNA. SOFT=0, 1, or 2 are available options to treat contacting entities. SFS and TSSFAC are the contact penalty factor and the time-step scale factor (see section 4.4), respectively. In addition, El=2 and 16 are two types of shell element formulation. The results show that energy absorbed can be considerably different (by approximately a factor of 2.5) due to various combinations of listed parameters.

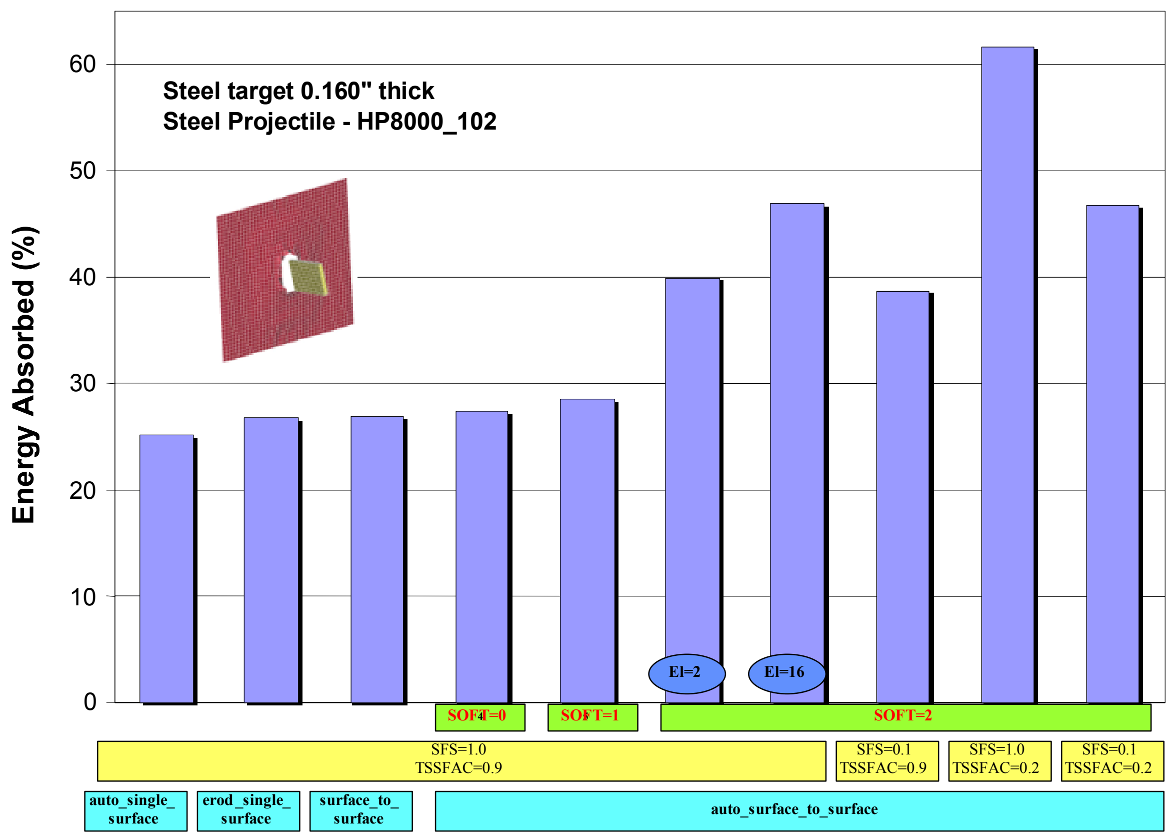

FIGURE 6-1. EFFECTS OF LS-DYNA CONTACT PARAMETERS (STEEL TARGET)

A limited parametric study was also performed on the ballistic test simulation of an eight-layer Zylon model (1x8) (see section 2.3), which also includes the user-defined fabric material model. As mentioned in section 2.4, the software version and the platform were kept the same throughout the current research program for consistency. The percent energy absorption for the baseline analysis was 19.4 percent, as shown in table 2-3. Figure 6-2 shows the effects on the results of the studied contact parameters and the element type; the middle column being the baseline analysis for which the results were acceptable when compared to the test results. To establish the variation on the result due to the computer platform only, the baseline analysis was also repeated on a different platform (IBM Unix workstation). The result was observed to be 20 percent less than the baseline using an HP Unix workstation. No other parametric combinations were studied.

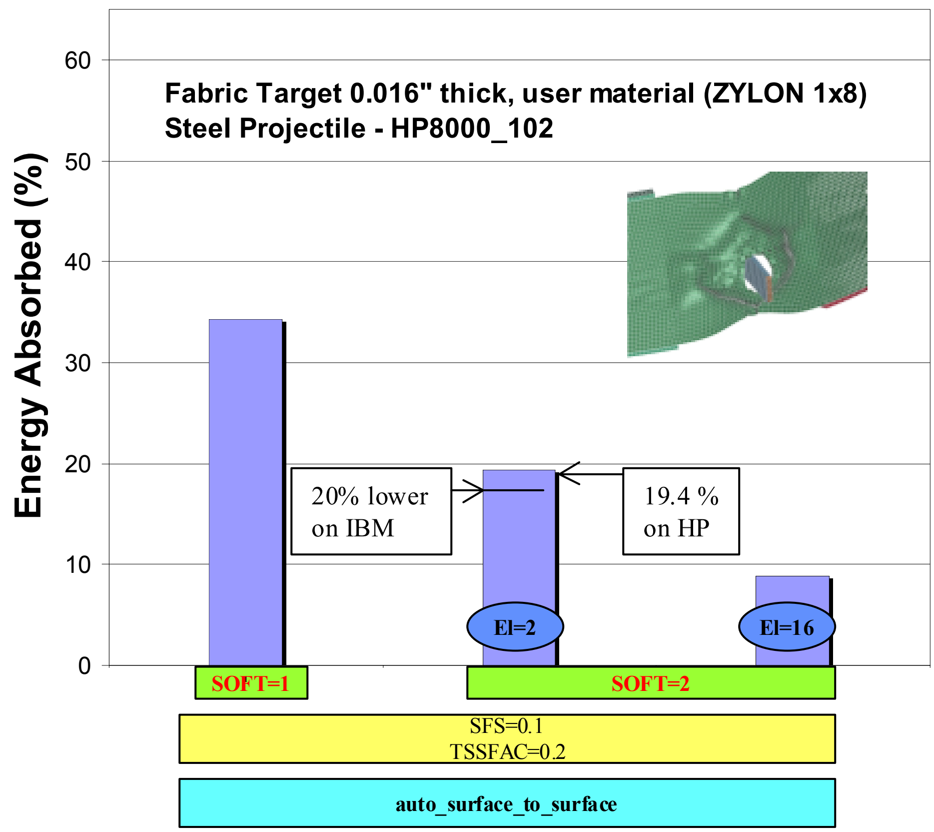

FIGURE 6-2. EFFECTS OF LS-DYNA CONTACT PARAMETERS AND PLATFORM (FABRIC TARGET)

7. CONCLUDING REMARKS.

This report contains numerical modeling of the engine containment ring ballistic tests conducted by NASA Glenn Research Center. LS-DYNA code was used for modeling. The material model used in this study was developed by SRI International. Modifications were made to the material model until a reasonable correlation was obtained between simulations and the test data. Subsequently, the resulting material model and modeling techniques were used to model and simulate a recent fan blade-out containment test of a full-scale Honeywell turbofan engine.

The following items summarize the overall conclusions of the work performed by Honeywell in this study:

- The new user-defined material model was successfully compiled within the LS-DYNA code. The same model is able to represent both Kevlar® and Zylon® material behavior, with separately provided, material-specific constants. The model formulation was based on actual material data and provides a more realistic representation of the fabric behavior. The new material model is independent of the number of fabric layers and, therefore, provides the flexibility to model single or multiple fabric layers.

- For the range of analytical parameters considered in this work, promising correlation was obtained between the simulation and the ballistic test results for both Kevlar and Zylon, using a single shell-element layer simulating all the fabric layers. Both energy absorption and overall deflection behavior of the fabric systems were successfully simulated. The relative simulations are able to depict the ballistic strength differences between Zylon and Kevlar. Similar successful analysis-to-test correlations were obtained when up to four layers of shell elements were used to model all fabric layers. Although good trends were observed up to four shell-element layers, the prediction capability was not satisfactory for modeling techniques using more than four layers. More work is needed to explore the limitations of modeling techniques involving a high number of shell elements.

- A full-scale engine fan blade-out event was successfully simulated using the fabric material models and developed analytical methodologies. Good correlation was obtained between the simulation and the engine containment test results, using the new Kevlar material model and the single shell layer modeling technique. The prediction capability was significantly improved with the new material model and the associated modeling techniques, with respect to the previous methodology used at Honeywell.

- In spite of successful results during the ballistic test simulations, further analytical enhancement with multilayer modeling was not possible due to numerical instabilities.

- Comparison of Kevlar and Zylon capabilities within the same containment design revealed containment results consistent with the ballistic test trends. For the same number of fabric layers, Zylon offers a weight reduction possibility if it is used in lieu of Kevlar.

- The mesh density was kept constant during this program, but the possible effects on the results was not investigated. Further investigation on mesh sensitivity, contact parameters, and multilayer numerical instabilities are recommended.

- The results showed that the choice of analysis parameters and solution algorithms, such as contact treatment, had a big effect on the resolution of the predictions. A brief discussion of the variations in the results that can be experienced using LS-DYNA, depending on the contact types, processor types, and computer platforms, was provided in section 6.
- Based on the experience gained during the execution of the impact and containment simulations, a generic containment finite element model, including fabric wraps, was created. The purpose of this model is to provide LS-DYNA users with generic guidelines for modeling composite fabric wraps in impact containment-related applications.

It is recommended that the following topics be examined in future work.

- Material model for alternative composite fabrics—Although ballistic testing on heavy Zylon was also performed by NASA, a model was not produced due to a lack of static material property data. The material model for this fabric can be derived with reasonably short effort and will help increase the validation database. Due to its high strength, this material offers a high potential for weight reduction in engine fragment containment applications.

- More representative fan blade release experiments—Ballistic experiments should be performed in which more representative tangential trajectory of the fan blade fragment is studied. This will facilitate the interpretation of the ballistic test results for potential use in containment design systems.

- Multiple shell-element layers to model multiple fabric plies—Efforts to investigate fabric impact simulations using multiple layers of shells to model thick fabric layers should be continued. This would provide the capability to indicate the number of layers penetrated versus the number of layers remaining during a containment event and, therefore, better evaluate the containment margin.

- Sensitivity to modeling parameters—The effects of the mesh sensitivity, various contact parameters, and other computational parameters should be further investigated.

- Simulation of more fan blade containment applications—The derived fabric material model should be used to simulate other engine fan blade containment systems. This would increase the confidence in adequately simulating different designs with the same methodology.

- LS-DYNA benchmarking for containment problems—Similar to crashworthiness industry applications, Livermore Software Technology Company should establish aerospace benchmark examples to ensure that LS-DYNA code predictions are consistent across platforms and future software versions.

8. REFERENCES.

1. Periera, M. and Revilock, D., "Explicit Finite Element Modeling of Multilayer Composite Fabric for Gas Turbine Engine Containment Systems, Part 2: Ballistic Impact Testing," FAA report DOT/FAA/AR-04/40,P2, 2004.

2. Simons, J., Erlich, D., and Shockey, D., "Explicit Finite Element Modeling of Multilayer Composite Fabric for Gas Turbine Engine Containment Systems, Part 3: Model Development and Simulation of Experiments," FAA report DOT/FAA/AR-04/40,P3, 2004.

3. Lesuer, D., "Experimental Investigation of Material Models for Ti-6Al-4V and 2024-T3," FAA report DOT/FAA/AR-00/25, September 2000.

4. Kay, G., "Failure Modeling of Titanium 6Al-4V and 2024-T3 Aluminum With the Johnson-Cook Material Model," FAA report DOT/FAA/AR-03/57, September 2003.

APPENDIX A—LS-DYNA USER INPUT FOR KEVLAR AND ZYLON MATERIAL MODEL

```
*KEYWORD
$ ------------------------------
$
$ DEFINITION OF MATERIAL     192  Zylon
$ ===================================================
$ === Zylon AS 35x35, 500 Denier
$     User-defined material model from FAA AACE Grant Project
$     fabric density = 1.54 g/cm^3 or 0.0556 lb/in^3
$     "model equivalent" density (x2)= 3.08 g/cm^3  or 0.1112
lb/in^3
$     LS-DYNA units:  0.1112 / 386.4 = 2.877E-04
$ ---------------------------------------------------
$
*MAT_USER_DEFINED_MATERIAL_MODELS
$      mid         ro         mt        lmc        nhv    iortho
ibulk        ig
       192  2.877e-4         47         48         15         1
1         1
$   card 2: ivect ifail
$    ivect     ifail
         0         1
$   card 3: aopt
$     aopt
       3.0
$   card 4:
         0         0         1
$     emod     epmin     epmax     sigmax    crimpx    crimpy
epsoft     ecrimp
     13.34    0.0250      .036    0.4205     0.037     0.006
0.01      0.047
$   comfac        g2        epc        epu    epfail     ddmax
tc
      .005       0.0     0.005     0.005      0.00       0.1
2.e-3        0.0
       0.0       0.0       0.0       0.0       0.0       0.0
0.0       0.0
       0.0       0.0       0.0       0.0       0.0       0.0
0.0       0.0
       0.0       0.0       0.0       0.0       0.0       0.0
0.0       0.0
       0.0       0.0       0.0       0.0       0.0       0.0
0.0       0.0
```

```
$
$ DEFINITION OF MATERIAL     292 Kevlar
$ ===================================================
$ === Kevlar 29 AS 17x17, 1500 Denier
$     User-defined material model from FAA AACE Grant Project
$     fabric density = 1.44 g/cm^3 or 0.052 lb/in^3
$     “model equivalent” density (x2)= 2.88 g/cm^3  or 0.104
lb/in^3
$     LS-DYNA units:  0.104 / 386.4 = 2.6915E-04
$ ---------------------------------------------------
$
*MAT_USER_DEFINED_MATERIAL_MODELS
$   card 1: mid    ro    mt  lmc  nhv  iortho  ibulk  ig
$      mid         ro         mt        lmc        nhv    iortho
ibulk        ig
       292   2.69e-4         47         48         15         1
1         1
$   card 2: ivect ifail
$   card 2: ivect ifail
         0         1
$   card 3: aopt
       3.0
$   card 4:
         0         0         1
$  card 5 - 10
$     emod     epmin     epmax     sigmax    crimpx    crimpy
epsoft     ecrimp
     10.15    0.0235    0.0262    0.3045     0.010     0.010
0.01     0.091
$   comfac        g2       epc        epu     epfail     ddmax
tc
      .005       0.0     0.005     0.005      0.00       0.1
8.e-3       0.0
       0.0       0.0       0.0       0.0       0.0       0.0
0.0       0.0
       0.0       0.0       0.0       0.0       0.0       0.0
0.0       0.0
       0.0       0.0       0.0       0.0       0.0       0.0
0.0       0.0
       0.0       0.0       0.0       0.0       0.0       0.0
0.0       0.0
$
```

APPENDIX B—BALLISTIC TEST DATA AND LS-DYNA SIMULATION RESULTS FOR KEVLAR AND ZYLON MATERIALS

TABLE B-1. LS-DYNA ANALYSIS RESULTS AND BALLISTIC TEST RESULTS FOR KEVLAR

		LS-DYNA Analysis						Ballistic Tests							Analysis Scaled to Tested Energy			
Model ID	Fabric Layers (n)	Shell Layers (k)	Analysis Impact Velocity (ft/sec)	Impact Energy (in-lb)	Exit Energy (in-lb)	Absorbed Energy (in-lb)	Absorbed Energy (%)	Test ID	Test Impact Velocity (ft/sec)	Projectile Mass (g)	Impact Energy (in-lb)	Exit Energy (in-lb)	Absorbed Energy (in-lb)	Absorbed Energy (%)	Impact Energy (in-lb)	Exit Energy (in-lb)	Absorbed Energy (in-lb)	Average Absorbed Energy (in-lb)
model231_1	1	1	388	19977	16133	3844	19.24	LG433	389	316.7	19703	17537	2166	10.99	19703	15912	3791	3738
								LG434	384	315.9	19151	16926	2225	11.62	19151	15466	3685	
model232_2	2	1	345	16040	6966	9074	56.57	LG444	349	316.4	15844	10053	5791	36.55	15844	6881	8963	8858
								LG449	345	316.2	15473	10119	5354	34.60	15473	6720	8753	
model222_4	4	1	904	110150	99656	10494	9.53	LG403	900	318.4	106033	93469	12564	11.85	106033	95931	10102	10205
								LG410	912	316.4	108195	97331	10864	10.04	108195	97887	10308	
model228_8	8	1	875	103030	83846	19184	18.62	LG404	897	317.8	105128	87640	17488	16.64	105128	85554	19575	18572
								LG409	888	316.0	102331	84819	17512	17.11	102331	83277	19054	
								LG424	834	320.9	91766	73029	18737	20.42	91766	74680	17087	
model230_16	16	1	896	108270	61487	46783	43.21	LG429	914	316.2	108601	67392	41209	37.95	108601	61675	46926	46282
								LG432	896	320.0	105620	55585	50035	47.37	105620	59982	45638	
model229_24	24	1	904	110150	29186	80964	73.50	LG405	898	319.0	105761	32265	73496	69.49	105761	28023	77738	77615
								LG411	886	314.8	101598	22076	79522	78.27	101598	26920	74678	
								LG427	915	317.9	109424	48315	61110	55.85	109424	28994	80431	

TABLE B-2. LS-DYNA ANALYSIS RESULTS AND BALLISTIC TEST RESULTS FOR ZYLON

		LS-DYNA Analysis						Ballistic Tests							Analysis Scaled to Tested Energy			
Model ID	Fabric Layers (n)	Shell Layers (k)	Analysis Impact Velocity (ft/sec)	Impact Energy (in-lb)	Exit Energy (in-lb)	Absorbed Energy (in-lb)	Absorbed Energy (%)	Test ID	Test Impact Velocity (ft/sec)	Projectile Mass (g)	Impact Energy (in-lb)	Exit Energy (in-lb)	Absorbed Energy (in-lb)	Absorbed Energy (%)	Impact Energy (in-lb)	Exit Energy (in-lb)	Absorbed Energy (in-lb)	Average Absorbed Energy (in-lb)
model122_4	4	1	891	107020	98175	8845	8.26	LG406	895	319.5	105220	91585.2	13635	12.96	105220	96524	8696	7793
								LG412	798	318.4	83361	70333.5	13027	15.63	83360	76471	6890	
model122_2	4	2	891	107020	96378	10642	9.94	LG406	895	319.5	105220	91585.2	13635	12.96	105220	94757	10463	9376
								LG412	798	318.4	83361	70333.5	13027	15.63	83360	75071	8289	
model122	4	4	891	107020	97055	9965	9.31	LG406	895	319.5	105220	91585.2	13635	12.96	105220	95423	9797	8780
								LG412	798	318.4	83361	70333.5	13027	15.63	83360	75599	7762	
model128_8	8	1	904	110150	88753	21397	19.43	LG408	904	318.0	106843	82008.5	24834	23.24	106843	86088	20755	20583
								LG413	901	319.9	106769	79198.9	27570	25.82	106769	86029	20740	
								LG417	892	314.6	102913	80926.9	21986	21.36	102913	82922	19991	
								LG425	908	316.6	107316	84140.4	23176	21.60	107316	86469	20846	
model128_4	8	2	904	110150	91430	18720	17.00	LG408	904	318.0	106843	82008.5	24834	23.24	106843	88685	18158	18008
								LG413	901	319.9	106769	79198.9	27570	25.82	106769	88624	18145	
								LG417	892	314.6	102913	80926.9	21986	21.36	102913	85423	17490	
								LG425	908	316.6	107316	84140.4	23176	21.60	107316	89078	18238	
model128_2	8	4	904	110150	90339	19811	17.99	LG408	904	318.0	106843	82008.5	24834	23.24	106843	87627	19216	19057
								LG413	901	319.9	106769	79198.9	27570	25.82	106769	87566	19203	
								LG417	892	314.6	102913	80926.9	21986	21.36	102913	84404	18509	
								LG425	908	316.6	107316	84140.4	23176	21.60	107316	88015	19301	
model128	8	8	904	110150	91643	18507	16.80	LG408	904	318.0	106843	82008.5	24834	23.24	106843	88891	17951	17803
								LG413	901	319.9	106769	79198.9	27570	25.82	106769	88830	17939	
								LG417	892	314.6	102913	80926.9	21986	21.36	102913	85622	17291	
								LG425	908	316.6	107316	84140.4	23176	21.60	107316	89285	18031	

TABLE B-2. LS-DYNA ANALYSIS RESULTS AND BALLISTIC TEST RESULTS FOR ZYLON (Continued)

		LS-DYNA Analysis						Ballistic Tests							Analysis Scaled to Tested Energy			
Model ID	Fabric Layers (n)	Shell Layers (k)	Analysis Impact Velocity (ft/sec)	Impact Energy (in-lb)	Exit Energy (in-lb)	Absorbed Energy (in-lb)	Absorbed Energy (%)	Test ID	Test Impact Velocity (ft/sec)	Projectile Mass (g)	Impact Energy (in-lb)	Exit Energy (in-lb)	Absorbed Energy (in-lb)	Absorbed Energy (%)	Impact Energy (in-lb)	Exit Energy (in-lb)	Absorbed Energy (in-lb)	Average Absorbed Energy (in-lb)
model130_16	16	1	904	110150	37645	72505	65.82	LG426	911	316.8	108094	51694.9	56400	52.18	108094	36942	71152	71152
model130_8	16	2	911	111840	58109	53731	48.04	LG426	911	316.8	108094	51694.9	56400	52.18	108094	56163	51932	51932
model130_4	16	4	911	111840	62208	49632	44.38	LG426	911	316.8	108094	51694.9	56400	52.18	108094	60125	47970	47970
model130_2	16	8	911	111840	70876	40964	36.63	LG426	911	316.8	108094	51694.9	56400	52.18	108094	68502	39592	39592
model130	16	16	830	106730	71246	35484	33.25	LG426	911	316.8	108094	51694.9	56400	52.18	108094	72157	35938	35938
model129_24	24	1	904	110150	1510	108640	98.60	LG407 LG414	904 830	316.1 315.9	106204 89472	0 0	106204 89472	100.00 100.00	106204 89472	1456 1227	104749 88245	96497
model129_12	24	2	904	110150	1266	108884	98.90	LG407 LG414	904 830	316.1 315.9	106204 89472	0 0	106204 89472	100.00 100.00	106204 89472	1221 1028	104984 88444	96714
model129_6	24	4	904	110150	1155	108995	99.00	LG407 LG414	904 830	316.1 315.9	106204 89472	0 0	106204 89472	100.00 100.00	106204 89472	1114 938	105091 88534	96812
model129_3	24	8	904	110150	34700	75450	68.50	LG407 LG414	904 830	316.1 315.9	106204 89472	0 0	106204 89472	100.00 100.00	106204 89472	33457 28186	72747 61286	67017
model129_2	24	12	904	110150	49365	60785	55.18	LG407 LG414	904 830	316.1 315.9	106204 89472	0 0	106204 89472	100.00 100.00	106204 89472	47597 40098	58608 49374	53991
model129	24	24	904	92840	50000	42840	46.14	LG407 LG414	904 830	316.1 315.9	106204 89472	0 0	106204 89472	100.00 100.00	106204 89472	57198 48186	49007 41286	45146

APPENDIX C—COMPARISON OF BALLISTIC TEST RESULTS AND LS-DYNA SIMULATION RESULTS FOR ZYLON MATERIAL

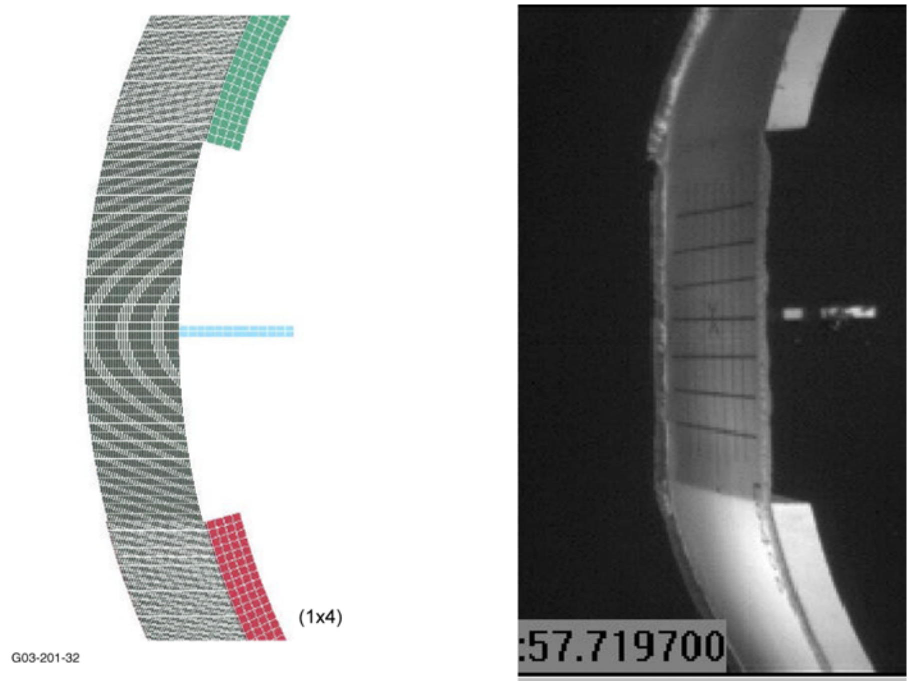

(a)

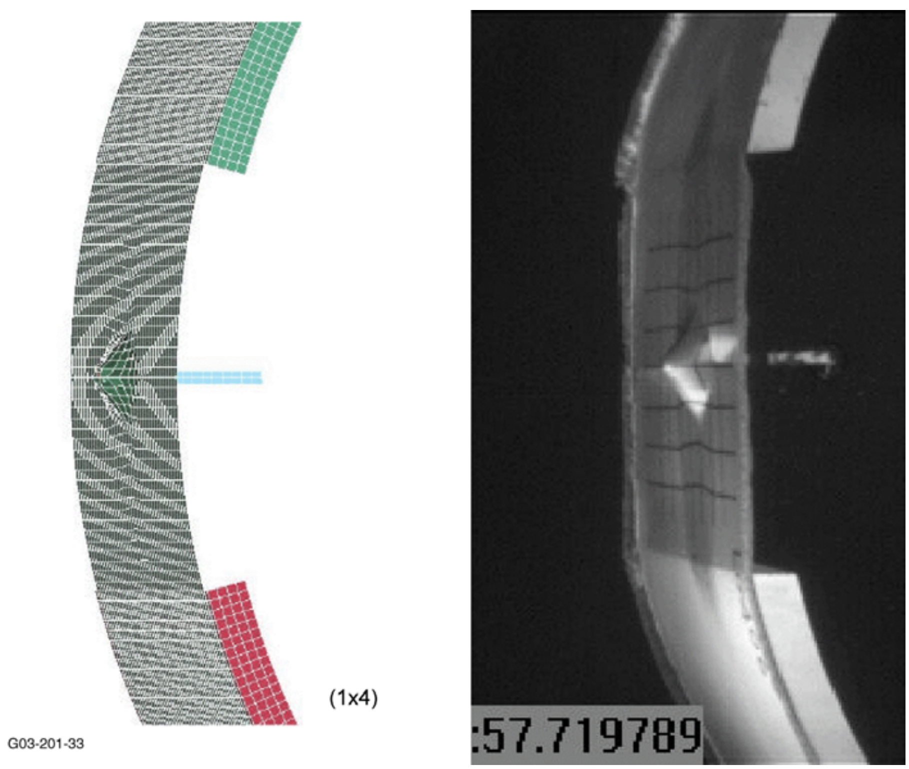

(b)

FIGURE C-1. ANALYSIS VS TEST FOR FOUR-LAYER ZYLON

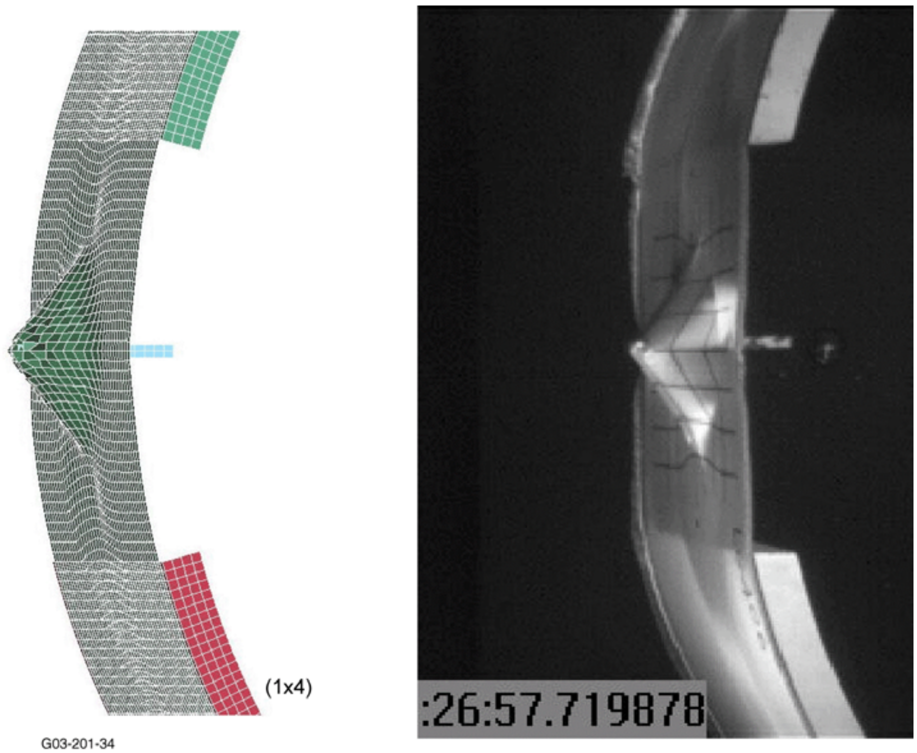

(c) G03-201-34

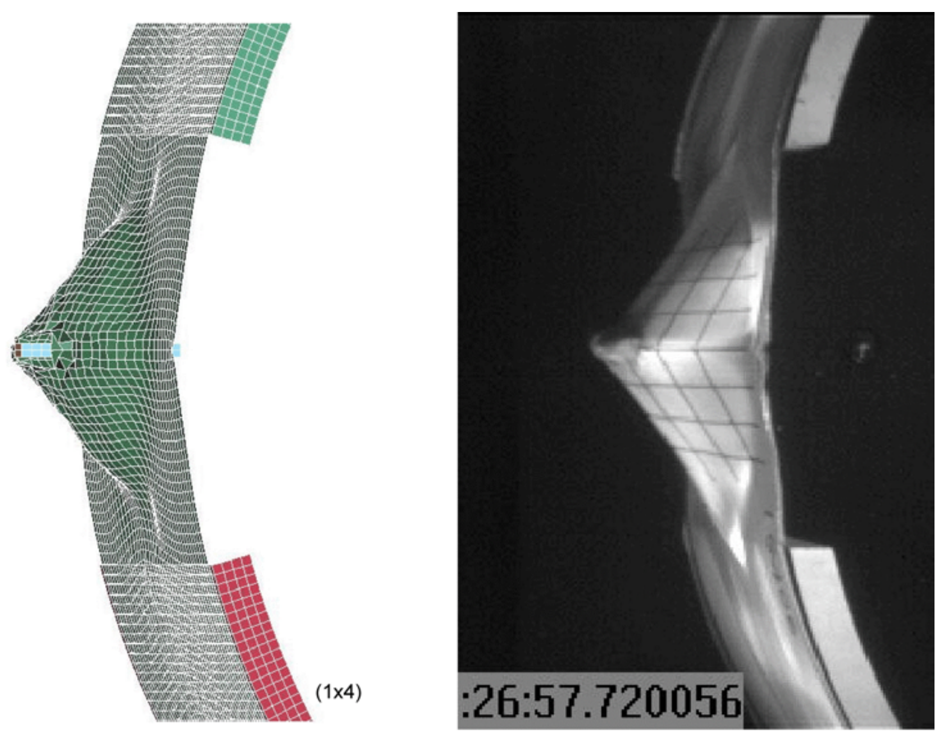

(d) G03-201-35

FIGURE C-1. ANALYSIS VS TEST FOR FOUR-LAYER ZYLON (Continued)

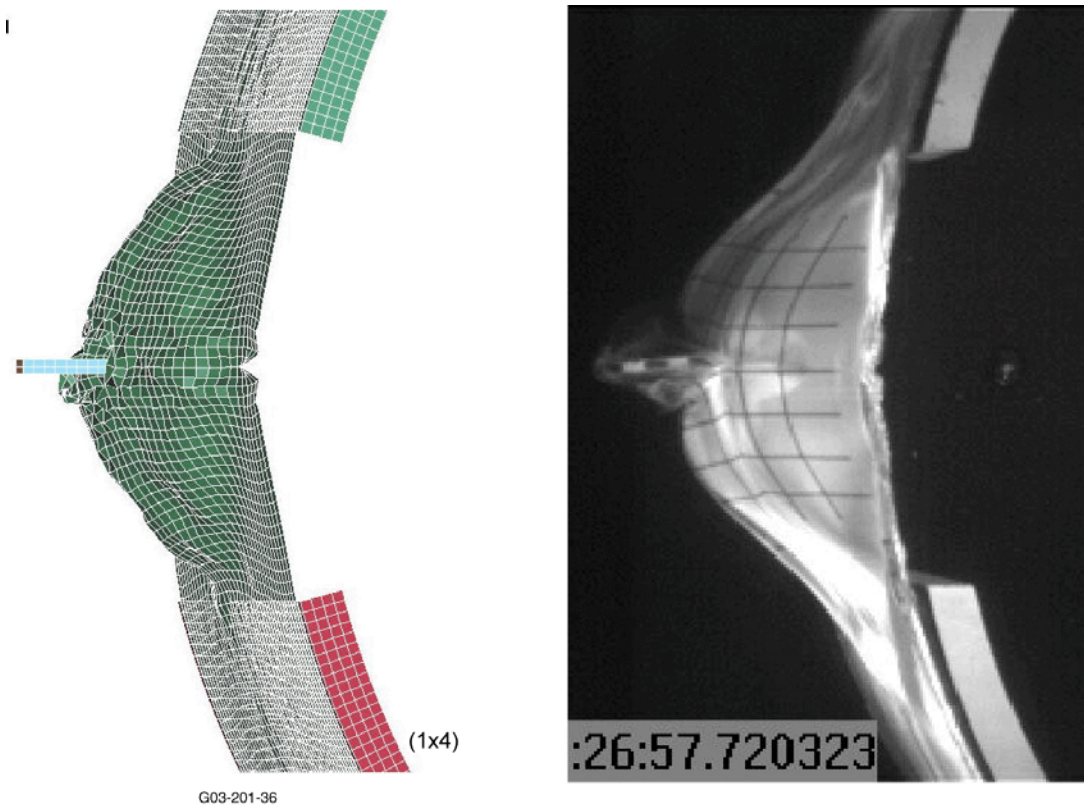

(e)

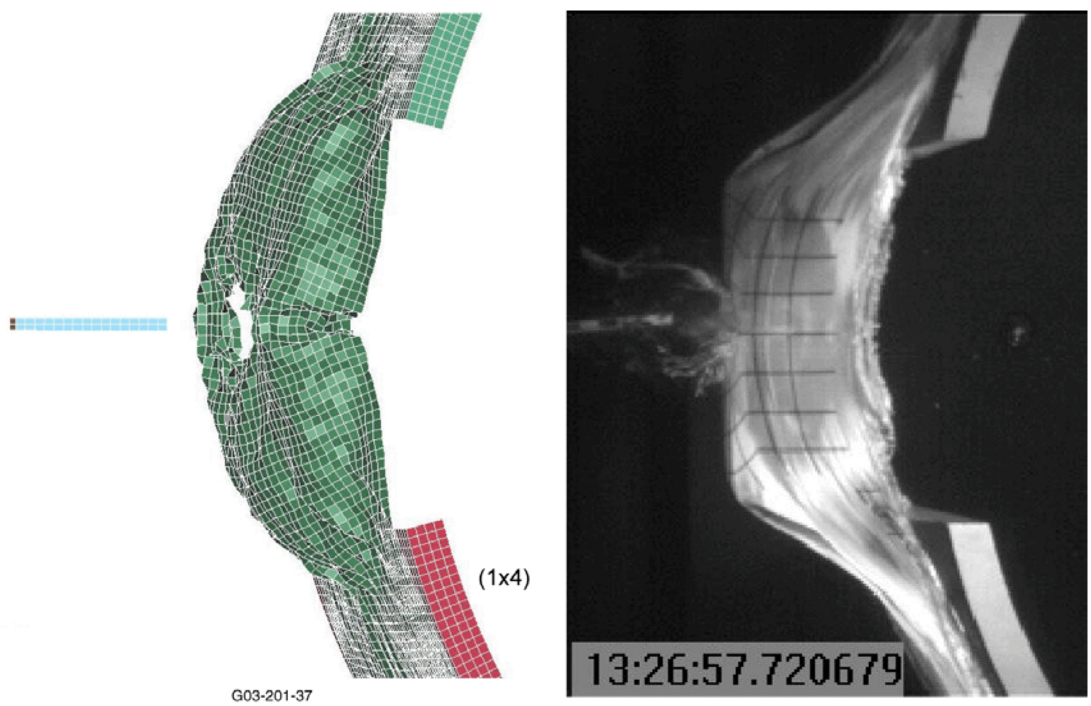

(f)

FIGURE C-1. ANALYSIS VS TEST FOR FOUR-LAYER ZYLON (Continued)

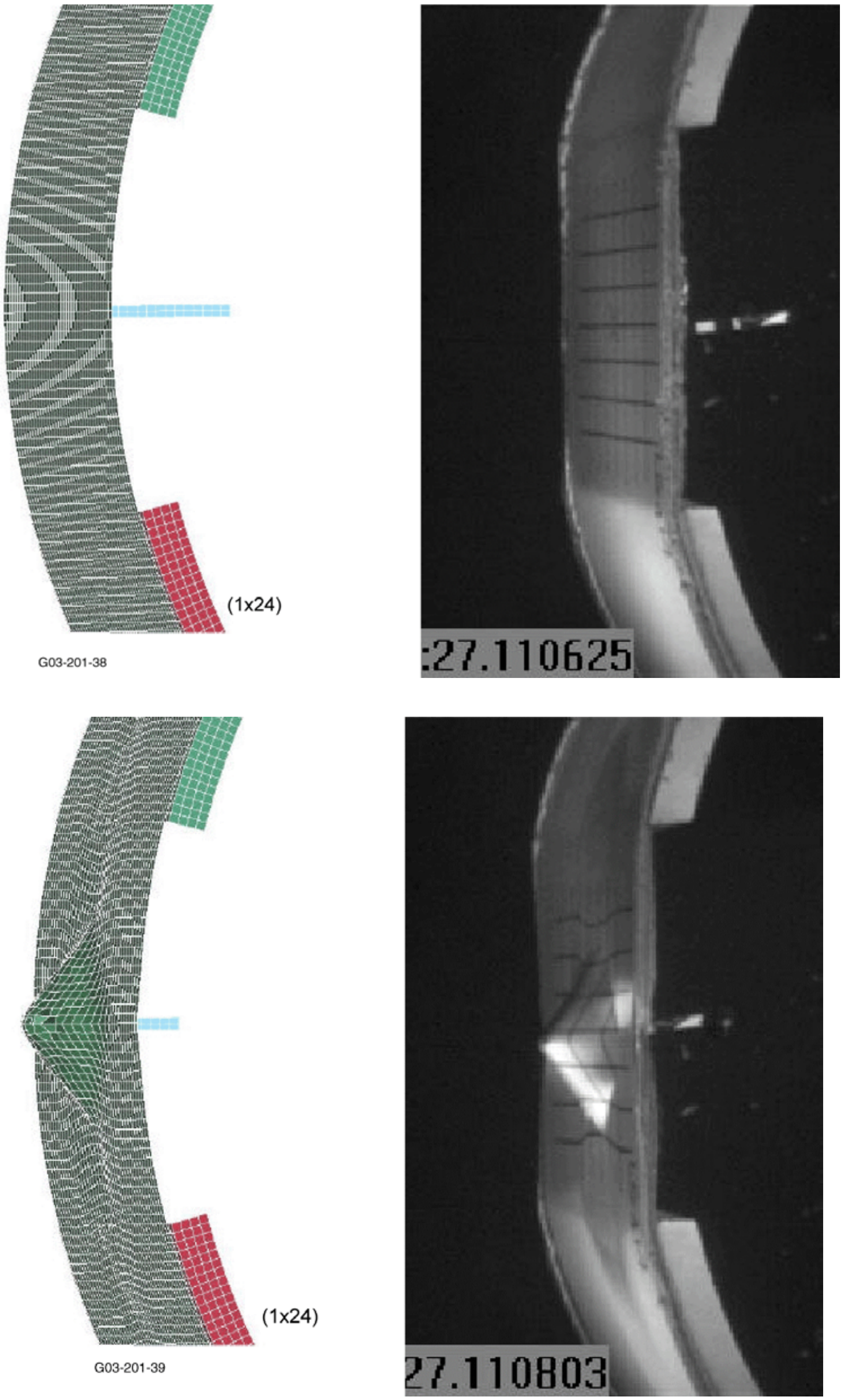

(a)

(b)

FIGURE C-2. ANALYSIS VS TEST FOR 24-LAYER ZYLON

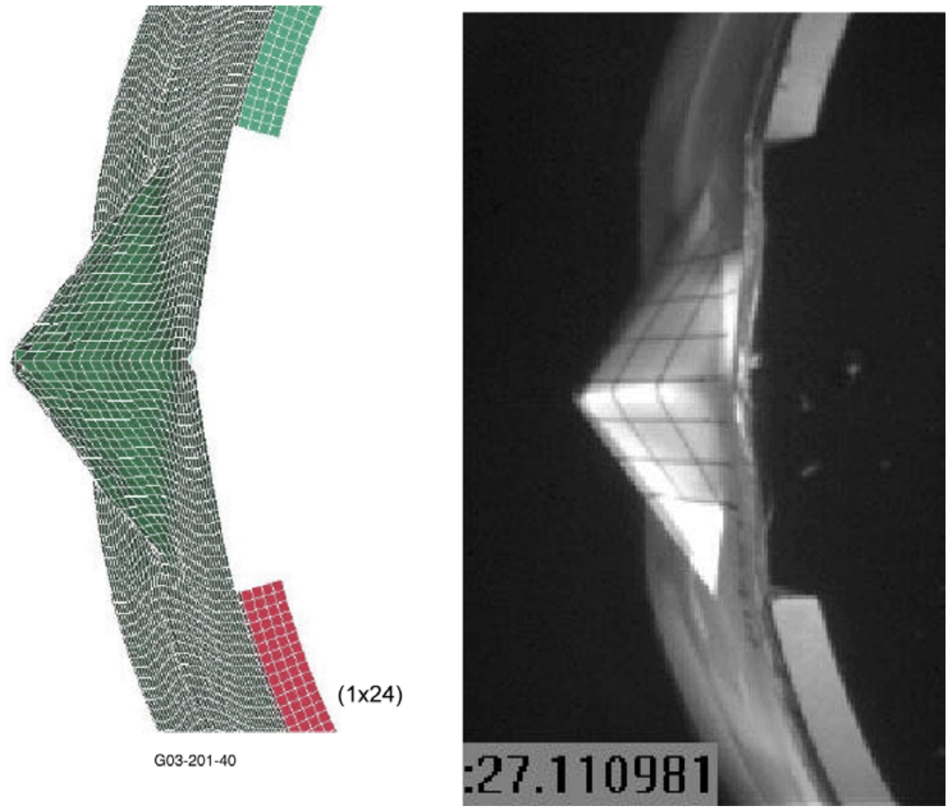

(c)

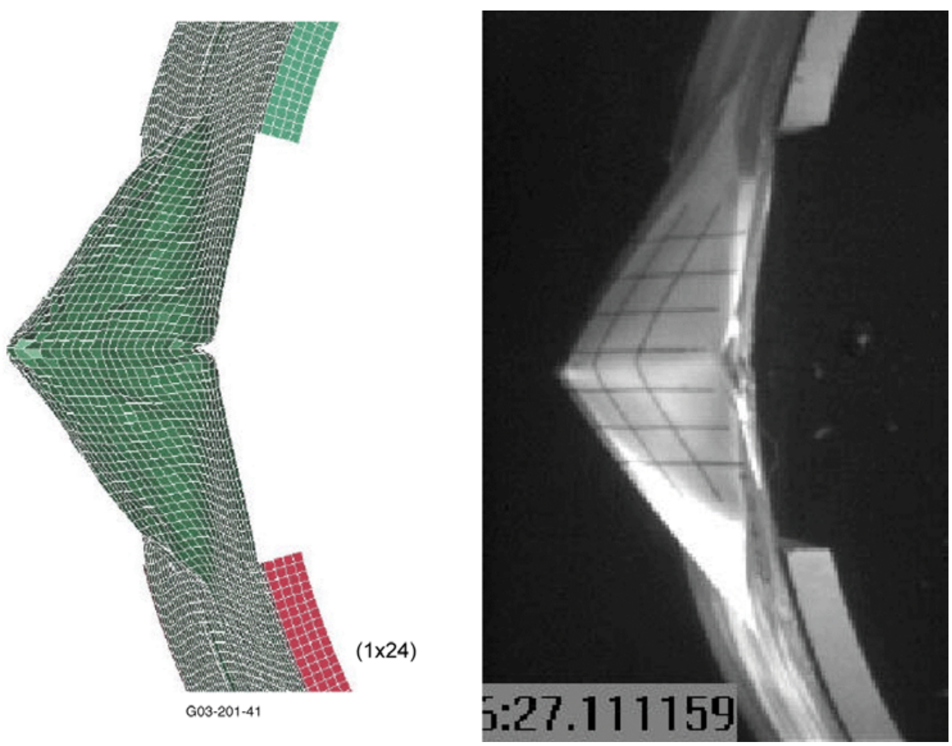

(d)

FIGURE C-2. ANALYSIS VS TEST FOR 24-LAYER ZYLON (Continued)

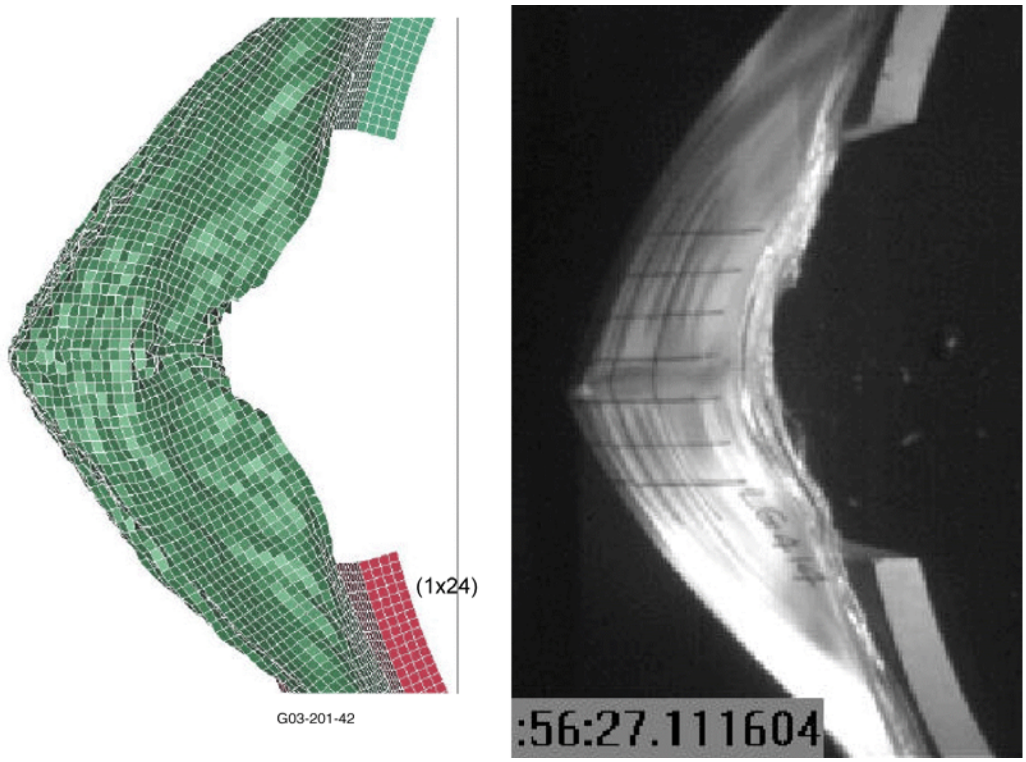

(e)

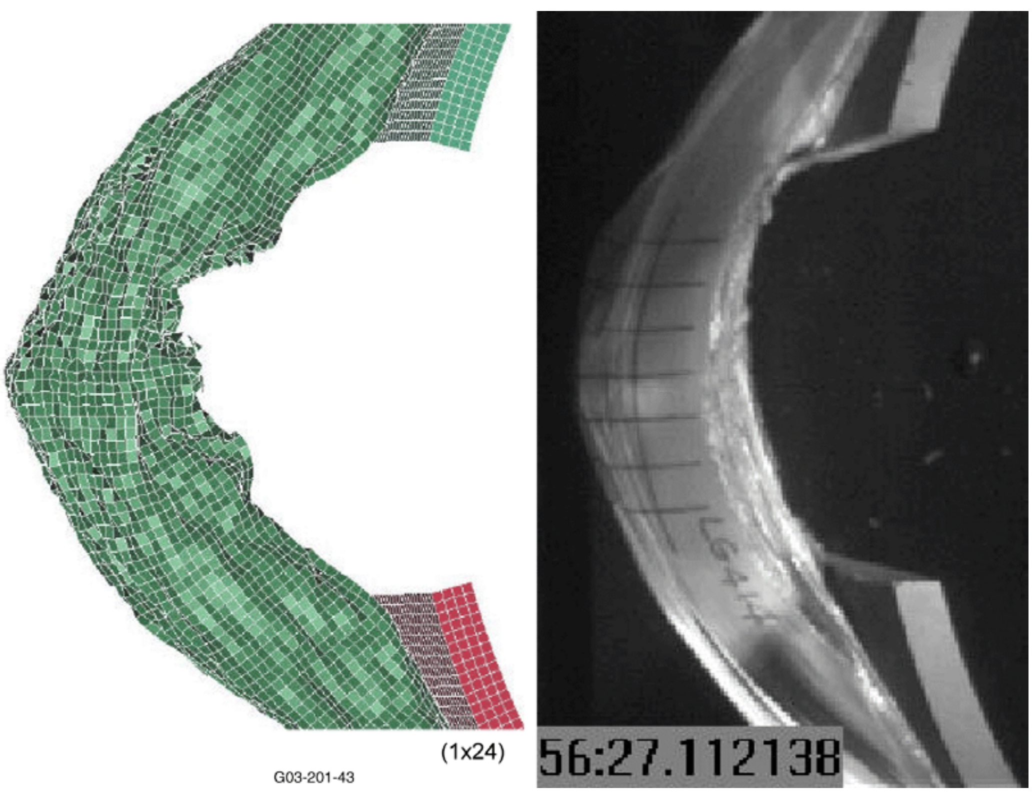

(f)

FIGURE C-2. ANALYSIS VS TEST FOR 24-LAYER ZYLON (Continued)